

Report 94.073
Neotectonic studies in the
Ranafjorden area, northern Norway

Report no. 94.073		ISSN 0800-3416	Grading: Open	
Title: Neotectonic studies in the Ranafjorden area, northern Norway				
Authors: Odleiv Olesen, Svein Gjelle, Herbert Henkel, Tor Arne Karlsen, Lars Olsen & Terje Skogseth		Client: Geological Survey of Norway, Nordland Programme		
County: Nordland		Commune: Mo i Rana		
Map-sheet name (M=1:250.000) Mo i Rana		Map-sheet no. and name (M=1:50.000) 1827 II Nesna, 1927 I Mo i Rana, 1927 IV Sjona, 2027 IV Storforshei,		
Deposit name and grid-reference:		Number of pages: 42		Price: 240,-
Fieldwork carried out: 1993 and 1994		Date of report: 30.11.94	Project no.: 61.2543.08	Person responsible: <i>Jan S. Reining</i>
<p>Summary:</p> <p>The Ranafjorden area in northern Norway is a region of increased seismicity and anomalous land uplift. There is evidence for recent movements in the bedrock; 1) A total of 0.89 m uplift of a bladder wrack mark from 1894 to 1990 in Hemnesberget; 2) Anomalous low uplift of the islands of Hugla and Tomma in the outer Ranafjorden area (0.0, 0.06 and 0.07 m from 1894 to 1990 compared to 0.25 - 0.30 m in the area to the north and the south); 3) Associated with the 1819 magnitude 5.8-6.2 earthquake in the Ranafjorden area, an uplift of a shallow sea floor above sea level during an aftershock was reported in the bay Utskarpen. During the main earthquake a major land slide occurred at the same location. This earthquake is the largest North European near-shore earthquake recorded in historical time; 4) An uplift of approximately 1 metre of a farmhouse in the 1870's at Båsmoen. The observation has been made relative to the two neighbouring mountains Snøfjellet and Høgtuva. 5) Approximately 0.5 m uplift of a boathouse in the bay Straumbotn during the last 50 years.</p> <p>A study of the postglacial overburden in the area has shown that deformations apparently occur more frequently than in the surrounding areas. The Båsmoen Fault, BF, lies within the regional Ranafjorden lineament and is a potential candidate for postglacial movements. The BF appears to consist of south-south-easterly dipping reverse-fault segments and can be traced for 50 km eastwards from the head of Sjona along Ranafjorden and further into the valley Dunderlandsdalen. The previously mentioned locations Utskarpen, Straumbotn and Båsmoen along the northern shore of Ranafjorden are situated on the fault and Hemnesberget is situated in the hanging-wall block 7 km to the south of the escarpment. Some 1 - 5-cm thick layers of fault gouge and steeply SSE-dipping fracturing were identified in the fault escarpments. The appearance of the fault is similar to the postglacial faults reported from the Lapland area in northern Fennoscandia. The height of the escarpment varies from 1 to 80 metres. Two separate swarms of N-S trending normal faults cutting the glacial morphology have been observed in the Nesna and Austerdalsvatn areas.</p> <p>There are, consequently, indications of recent faulting in the Ranafjorden area. It is, however, difficult to find conclusive evidence for postglacial and present-day movements along specific faults. We have therefore established a Global Positioning System (GPS) network designed to measure the active geological strain in the area.</p>				
Keywords: Geofysikk		Landhevning		Forkastning
Berggrunnsgeologi		Seismologi		Holocen
Kvartærgeologi		Fossil		Fagrapport

CONTENTS

1 INTRODUCTION	4
2 GEOLOGICAL SETTING	5
3 NEOTECTONICS	5
3.1 Seismicity	5
3.2 <i>In situ</i> stress measurements.....	6
3.3 Land uplift.....	7
3.4 Late Quaternary faults	8
3.5 Small-scale brittle faults	9
3.6 Deformation of postglacial sediments.....	9
3.7 Båsmoen Mine.....	10
3.8 Carbonate-cemented pillars on Nesøya.....	11
3.9 GPS network.....	12
4 DISCUSSION AND CONCLUSIONS	13
5 ACKNOWLEDGEMENTS.....	14
6 REFERENCES	15
List of figures	19

Odleiv Olesen, Svein Gjelle & Lars Olsen, Norges geologiske undersøkelse, P.O.Box 3006, N-7002
Trondheim, Norway

Herbert Henkel, Kungliga Tekniska Högskolan, S-100 44 Stockholm, Sweden

Tor Arne Karlsen & Terje Skogseth, Norges tekniske høgskole, N-7034 Trondheim, Norway

1 INTRODUCTION

New data on Late Quaternary faults (Fig. 1), land uplift and earthquake distribution show that the bedrock of Fennoscandia locally is less stable than earlier anticipated. Opinions differ on the age of formation of the different postglacial faults; from formation immediately after deglaciation in northern Sweden (Lagerbäck 1992) to present-day active faulting in southwestern and northern Norway (Anundsen 1989, Olesen et al. 1992b). There are numerous sharp lineaments representing potential postglacial faults along the coast of Norway. It is, however, very time consuming to map these lineaments to check if they represent young faults. The situation in the Lapland area where most postglacial faults have been found so far, is much simpler. Escarpments which were older than the glaciation, were covered with till and consequently do not interfere with the young escarpments cutting through the overburden. Limited erosion due to the gentle topography and little precipitation has also tended to preserve the escarpments better than in the coastal areas. In the search for postglacial faults it is, therefore, necessary to limit the area of investigation. This can be achieved by locating the geological environment where the faults are most likely to occur. Studies of the postglacial Stuuragurra Fault in the Precambrian of Finnmark showed that postglacial faulting occurs in areas of: 1) increased seismicity (Olesen 1988), 2) regional zones of weakness (Olesen et al. 1992a) and 3) anomalous land uplift (Olesen et al. 1992b). When studying regional data-sets on seismicity (Bungum et al. 1991), land uplift (Sørensen et al. 1987, Bakkelid 1989, 1990, 1991 and 1992) and Landsat lineament analysis (Gabrielsen & Ramberg 1979a, Gabrielsen et al. 1981), the Ranafjorden area was found to be potentially the most favourable area for finding new postglacial faults in northern Norway. The existence of regional lineaments is also visible from the study of digital topography (Fig. 2). After defining the Ranafjorden area as the most promising target, a total of four weeks of fieldwork was carried out in August 1993 and August 1994 to locate potential postglacial faults.

2 GEOLOGICAL SETTING

The Ranafjorden area is underlain by the Rødingsfjell Nappe Complex (Figs. 3 & 4) to the north and east and the Helgeland Nappe Complex to the south and west (Gustavson & Gjelle 1991). The dominating lithologies of the nappe complexes are gneisses, mica schists and marbles. The tectonic basement windows, Sjona and Høgtuva, consisting of granitic gneisses, are situated to the north of the fjord while the Bindalen Batholith, comprising young Caledonian granites, is situated to the south. The rocks have been exposed to Caledonian deformation and metamorphism.

The dominant regional ice movement during the last glaciation in the Ranafjord area was directed westwards. During later stages of glaciation the ice movement in the Båsmoen area was directed towards the SSE. It is not known whether this latter ice movement was connected with calving in Ranafjorden during deglaciation, or alternatively if it may derive from an ice culmination developed during the later stages of glaciation in the Svartisen area.

3 NEOTECTONICS

3.1 Seismicity

Norway and nearby offshore areas have a low to moderate seismicity (Bungum et al. 1991), comparable with that in other intraplate regions such as eastern North America. The coastal zone of Nordland (Fig. 6) and the passive continental margin are seismically relatively active areas in northern Norway. The seismicity during the period 1987-1993 (Byrkjeland in prep.) shows many earthquakes occurring in the areas to the east and west of Svartisen and to the east of Ranafjorden (Fig. 6). The magnitude of these earthquakes is 2-3. The 1819 earthquake (magnitude 5.8-6.2) is situated within the Ranafjorden area and is the largest North European near-shore earthquake of the past few centuries (Muir Wood 1989). The effects of the earthquake were quite dramatic (Fig. 7) and it was followed by an extensive aftershock sequence. The event caused widespread damage to the foundations and chimneys of wooden buildings as well as very extensive rockfalls, liquefaction phenomena and a variety of disturbances in fjords and in the sea (Heltzen 1834, Muir Wood 1989). The spectacular earthquake swarms (Fig. 6) on Meløy (Bungum & Husebye 1979, Bungum et al. 1979, Vaage 1980) and Steigen to the north of Bodø (Atakan et al. 1994) are also located within the seismicity zone of the Nordland coast. The two swarms occurred in 1977/1978 and 1992 and contained 10,000 and 200 shocks, respectively, but no main shock was recorded. The magnitude of the shocks was up to 3.2 and 3.6, and the distance from Ranafjorden to the locations of the two swarms is 60 and 160 km, respectively. Earthquake swarms usually occur

in volcanically or tectonically active areas such as plate boundaries but have also been reported from passive continental margins surrounding the northern part of the Atlantic Ocean and the Arctic Sea (Atakan et al. 1994). These swarms may be interpreted to be related to the formation of new zones of weakness in relatively competent bedrock (R. Muir Wood, pers. comm. 1993).

The strike trend of the main active faults within the Meløy swarm (Fig. 6) was N20°-35°E and the dip was 60°SE (Bungum & Husebye 1979, Gabrielsen & Ramberg 1979, Vaage 1980). The faulting had a large component of normal fault motion and a minor component of right-lateral strike-slip (Fig. 6). Significant deviations (Fig. 6) from this fault orientation were also recorded (Vaage 1980). The strike trend of the composite fault plane solution (NE-SW) for the Steigen events (Atakan et al. 1994) is the same as that of the Meløy fault plane. Although the dip direction is different considerably (i.e., oblique-slip fault with a normal component dipping NW), both sets might be ascribed to the same stress situation.

3.2 *In situ* stress measurements

Regional principal stress directions show an overall tendency to trend N-S or E-W in northern Norway and NE-SW or NW-SE in southern Norway (Myrvang 1993). Fig. 6 shows that the *in situ* stress measurements made by Myrvang (1993) suggest deviations from the general N-S and E-W trends and that this phenomenon is most likely due to local fault complexities and topography. The horizontal stress magnitude is higher than that expected from the effect of the overburden. The Nordland and Vestlandet areas display the largest horizontal stresses in Norway and are also characterised by increased seismicity (Bungum et al. 1991). The maximum horizontal stress in the Ranafjorden area is higher than 20 MPa at moderate depths of 200-800 m and causes exfoliation in natural and man-made cuttings and spalling in tunnels (Myrvang 1993, Arne Myrvang, pers. comm. 1994). In the Kobbelv/Tysfjord area, which is situated 200 km to the north of Ranafjorden, rock bursting and buckling are observed at the surface (Myrvang 1993). The maximum compressive stress as derived from focal mechanism solutions (Bungum & Husebye 1979, Vaage 1980, Bungum et al. 1991) of the 1977/1978 earthquake swarm on Meløy reveals general N-S and E-W trends for the stress field (Fig. 6).

3.3 Land uplift

There is ample evidence for recent movements in the Ranafjorden area;

- 1) A total of 0.89 m uplift of a bladder wrack mark from 1894 to 1990 (Bakkelid 1990) in Hemnesberget. This observation represents an average annual uplift of 9.2 mm (Figs. 4 & 6), which is similar to the present maximum uplift of Fennoscandia in the Bay of Bothnia due to glacial rebound.
- 2) Three measurements of uplift of acorn barnacle and bladder wrack marks on the islands of Hugla and Tomma (Fig. 6) in the outer Ranafjorden area show anomalous low land uplift from 1894 to 1990 (0.0-0.07m) compared with the uplift recorded (0.23-0.30 m) to the north and to the south (Bakkelid, 1990, 1991). Fig. 6 shows average annual uplift in mm.
- 3) Associated with the 1819 magnitude 5.8-6.2 earthquake (Muir Wood 1989) in the Ranafjorden area, (see Chapter 3.1), Heltzen (1834) reported an uplift of the shallow sea floor above sea-level during an aftershock in the bay Utskarpen. During the main earthquake a major landslide occurred at the same location.
- 4) An uplift of approximately 1 metre of a farmhouse at Båsmoen in the 1870's (Grønlie 1923). The observation is made relative to the two neighbouring mountains Snøfjellet and Høgtuva. In the Båsmoen area, 6 out of a total of 7 breaks of water supply pipes during 1993 occurred within a circle of 250 m radius around this farmhouse (A. Hauknes, pers. comm. 1994). The cause of these breaks is not known. The densely built-up area of Båsmoen covers a region of 2 x 1 km.
- 5) A boat-house is also reported to have been uplifted c. 0.5 m during the last 50 years in the Straumbotn area (P. Straumfors pers. comm. 1994). This location is situated between Utskarpen and Båsmoen (Fig. 6).

These observations may be related to faults along Ranafjorden but originally some of them were attributed to other causes: 1) Changing marine conditions in Ranafjorden (Bakkelid 1990); 3) Piling up of material behind a rotational slump in the marine clay (Muir Wood 1989); 4) Uplift of the mountain Høgtuva (Grønlie 1923). The interpretation of Grønlie (1923) is, after all, a recognition of neotectonic activity and his version cannot totally be ruled out. A third, alternative interpretation of his observation is subsidence of Snøfjellet, which is situated almost exactly half-way between Båsmoen and Høgtuva. The subsidence of Snøfjellet only has to be a half of the possible uplift at Båsmoen or Høgtuva. Moreover, a combination of movements at either two or all three localities cannot be ruled out.

3.4 Late Quaternary faults

Deep NNE-SSW trending clefts on the Kvasshaugen mountain ridge between the valleys of Beiardalen and Gråtådal to the north of the Svartisen glacier were described by Grønlie (1939) and Johnsen (1981). The clefts are up to 4 m wide and 10 m deep and the eastern side is downfaulted (Figs. 4 & 6). These faults are interpreted to be of postglacial age and could be the result of a WNW-ESE oriented extension. The faults are classified as some of the most reliable claims of neotectonic surface fault rupture in Scandinavia (Muir Wood 1993).

The Båsmoen Fault, BF, lies within the regional Ranafjorden lineament which is a zone of increased seismicity (Bungum et al. 1991) and anomalous land uplift (Bakkelid 1990) and is a potential postglacial fault (Figs. 9,10,13-16). The westernmost section of the fault is situated within the lower units of the Rødingsfjell Nappe Complex, the Tjørnrasta and Straumbotn Nappes, whereas the easternmost section lies within the upper units, the Ramnålia and Plura Nappes (Søvegjarto et al. 1988, 1989). The BF generally cuts the strike of the foliation at a low angle (0-30°). It consists of SSE-dipping (40-70°) reverse faults segments and can be traced for 50 km eastwards from the head of Sjona Fjord along Ranafjorden and further east into the valley Dunderlandsdalen. The WSW-ENE trending fault zone is locally composed of 2-3 parallel escarpments within a 2-3 km wide belt (Fig. 5). The strike of the individual segments varies between N60°E and N110°E. The dip of the foliation along the fault is 20-60° towards the SSE. The foliation tends to be steeper in and adjacent to the fault scarp.

The localities Utskarpen, Straumbotn and Båsmoen on the northern shore of the Ranafjorden are situated along the fault (Figs. 4 - 6), whereas Hemnesberget is situated in the hanging-wall block 7 km to the south of the escarpment. An extension of the Båsmoen Fault may continue in the sound immediately to the north or to the south of the islands of Hugla and Handnesøya. All these locations show anomalous land uplift (see Chapter 3.3). We have, however, not yet found any conclusive evidence for postglacial movements along specific fault scarps.

Some 1-5 cm-thick layers of fault gouge and steeply dipping fractures were identified along the fault escarpments. The appearance of the fault is similar to that of the postglacial faults reported from the Lapland area of northern Fennoscandia (Lundquist & Lagerbäck 1976, Bäckblom & Stanfors 1989, Olesen et al. 1992b). The heights of the escarpments vary from 1 to 80 metres (Figs. 9, 13 - 16). We do, however, believe that a significant portion of these escarpments was formed before the last deglaciation since ice striae are observed locally along the escarpments. Detailed mapping of geological boundaries across the BF on Slettefjellet and Båsmofjellet shows that the maximum accumulated displacement is in the order of 5-10 m.

Two separate swarms of N-S to NNE-SSW trending normal faults cutting the glacial morphology have been observed in the Nesna (Fig. 19) and Austerdalsvatn (Fig. 20) areas and may be Riedel shears to the reverse fault. The western blocks are down-faulted.

3.5 Small-scale brittle faults

A number of small-scale faults occur in road-cuts between Straumbotn and Alteren in the hanging-wall block of the BF (Fig. 8). Four strike trends are recorded, of which NNE-SSW (N200°E) is the most frequently occurring. The dip of the fault planes varies but is generally about 60° towards the WNW. Three other trends are N80°E/30°S, N145°E/30°SW and N330°E/20°NE. The 080° trend coincides with the trend of the BF. All of these faults show 1-5-cm wide zones of fault gouge or intense fracturing. Quartz commonly occurs as a filling in these zones. The 200° trend is also frequently represented in the area by a steeply dipping fracturing. The age of the faults, however, is not known. We were generally unable to observe the amount of movement along the fault gouge zones because of lack of proper reference structures. In one locality, however, an apparent movement of 0.25 m could be detected and we expect the movement along the other faults to be of the same order of magnitude. Mapping of joints and faults at Utskarpen shows a similar distribution of trends (Fig. 12).

Fig. 11 shows rose diagrams and a stereoplot of the joints and faults within the Straumbotn-Båsmoen area which includes the central section of the Båsmoen Fault scarp. The main trends are N000-010°E and N070°E. Gabrielsen & Ramberg (1979a) and Gabrielsen et al. (1981) carried out an analysis of Landsat satellite images from the Helgeland area. The most pronounced trends in the Ranafjorden area were SW-NE and WSW-ENE. The N-S trend is less prominent on these regional data-sets but is distinguished in the detailed analysis of the Meløy area (Gabrielsen & Ramberg (1979b).

3.6 Deformation of postglacial sediments

Machine excavated sections in an erosional mound in postglacial sediments at Little Alteren (Fig. 22) were examined during August 1994. The location of the mound is within the zone of the Båsmoen Fault system and some 250 m north of a major fault line. The top of the mound is c. 30-32 m a.s.l. and the stratigraphy comprises about 5 m of bedded fluvial sand overlying marine clayey silt. Several steep faults were observed in the sections (Fig. 22), and the strike of the dominant fault planes varied between N-S and NE-SW with dip ranging from 20° to 70° to the NW. This accords well with an avalanche movement direction of the underlying marine deposits towards former river channels in the west and northwest, but not towards the present

river valley in the east and southeast. It is quite possible, although not yet proven, that this severe deformation occurred during an earthquake, with enhanced trembling or movement along the BF system. Indications of this exist. For instance, similar but not so well-developed corrugations in fine-grained sand are seen in postglacial sediments along another fault showing evidence of postglacial tectonic activity (Fig. 21) in the mound at Litle Alteren. It is therefore most likely that the sand deposits were shaken very violently in a water-saturated condition during deformation. The corrugated sand and the faulting of rusty horizons in the sand indicate that the sea-level was (lowered) below c. 25 m above present sea-level when the deformation event happened. This gives a maximum age of the event at c. 5,000 years B.P. A minimum age for this event is given by soil development of non-faulted slope deposits overlying faulted sand in the slope of the mound facing the present river valley in the southeast.

Such soil profiles need several hundreds of years to develop, and the deformation must therefore have occurred at least 1000 years ago. This agrees well with the requirements of water saturation during corrugation of sand in the mound, suggesting a deformational event not much later than 3000-4000 years ago, which is our best age estimate until absolute dates are available.

3.7 Båsmoen Mine

The Båsmoen Mine was in operation from 1893 to 1937 (Bøckman 1964) with intervals of standstill in the mining due to strikes and periods of recession. The deposit is situated within the Plura Nappe in the Rødingsfjell Nappe Complex (Søvegiarto et al. 1988) and consists of several ruler-shaped bodies of massive pyrite. The host rock is a highly brecciated and chloritised schist (Nordenskjöld 1895, Foslie 1926, Hofseth 1939 and Vogt 1939). The brecciation was formed during the mineralisation. The Båsmoen ore deposit is cut by the Båsmoen Fault which constitutes a reactivation through the much older fault breccia. Zones of fault gouge can be observed in an open pit and have also been reported earlier by Nordenskjöld (1895) and Søvegiarto (1978). The mine collapsed along the BF in 1913 and the deeper sections of the mine were abandoned due to mud and water pouring into the mine along the rock-slide continuing all the way from the surface (Bøckman 1964). The deeper part of the mine, which continued down to 65 m below sea level was never reopened.

Grønlie (1978) reported 2800 ± 90 ^{14}C -years old fossil vegetation in an open pit within the Båsmoen Mine. We think that this age is not the age of the fossils, but rather the age of subsequent recrystallisation and cementation in their host tufa-like sediments. The fossils occur along an approximately 500 m-long zone along the BF from the foot of the open pit westwards towards the hill Båsmofjellet. The occurrence of the fossils was attributed to water transport (Grønlie 1978); but they occur in a strongly lithified iron- and carbonate-rich tufa and such deposits are found only in connection with spring waters. The fossils consist of bark,

trunks, branches, cones, leaves, grass, etc. and are partly lying adjacent to and partly within the fault zone. We have not been able to relate the preservation of these fossils directly to movements along the BF, but the spring system which is required to explain the existence of the tufa which hosts the fossils may well be a result of fault activity along this zone.

It is also interesting to note the reported occurrence of a spring along the BF at Kildehaugen (Heltzen 1834), which may have been the same as that mentioned above. Such springs occur in many places along the postglacial faults in northern Fennoscandia (Lundquist & Lagerbäck 1976, Olesen et al. 1992a), indicating extensive systems of open fractures in the bedrock. Kildehaugen lies within the mining area at Båsmoen and the spring does not exist today. We would also like to point out that karst caves occur more commonly in the Rana area than in similar areas of abundant metalimestone bedrock. This phenomenon is, for instance, evident on the maps of karst landforms of Nordland and Troms by Lauritzen (1991a,b). What we do not know, however, is whether this apparent high frequency of karst merely is the result of more intensive exploration in the Rana area as compared to the other areas (A. Grønlie, S.E. Lauritzen, pers. comm. 1994).

3.8 Carbonate-cemented pillars on Nesøya

Nagy & Dypvik (1984) have described some spectacular pillar-like structures of lithified shell gravel up to 1.6 m in height occurring on a raised beach on Nesøya situated 20 km to the northwest of Lurøya (Fig. 4). Radiocarbon datings and fossil content show that the bioclastic constituents of the gravel were formed during the Holocene (two datings show ages of $6,880 \pm 80$ and 7190 ± 110 ^{14}C -yrs. B.P.), and that the cementation took place during the Subatlantic stage (two datings show that the cementation occurred later than $2,350 \pm 90$ and $2,780 \pm 170$ ^{14}C -yrs. B.P.). Nagy & Dypvik (1984) ascribed the formation to precipitation of a high-Mg calcite cement during periodical wetting and desiccation of the sediments, which occurred due to the postglacial elevation of the shallow-water carbonate blanket into the shoreface and foreshore, where it was subjected to erosion by wave and tidal action.

Hovland (1985) questioned this interpretation, mainly because the proposed process would have formed benches and terraces on the beach, not local mounds. He proposed an alternative model including an artesian supply of carbonate-rich solutions through cracks and fissures in the underlying bedrock. Nagy & Dypvik (1985) rejected this model since no artesian system can be found and if one had existed it would anyway have not been carbonate-rich since the bedrock consists exclusively of pyroxene-quartz monzonite and pyroxene monzonite.

The widespread neotectonic activity in the Helgeland area may offer an alternative model for the formation of the pillar-like structures on Nesøya and ought to be considered during any

eventual further studies. Strong earthquakes cause vibrations in the water-saturated sediments below the sea bottom and liquefaction phenomena are likely to occur, as described e.g. by Heltzen (1834) and Lagerbäck (1990) in association with the 1819 earthquake in the Ranafjorden area and the large post- or late-glacial earthquakes in northern Sweden, respectively. Repeated shaking of the sediments and flow of Mg-rich water through the porous shell gravel could have cemented the gravel and at the same time a mud volcano could then have accumulated on the sea bottom. When the blanket of sediments was eventually uplifted, all the sediments except the necks of the mud volcanoes would have been removed. This model could also explain why the cement content is highest in the uppermost section of the pillars. The age of the cementation coincides approximately with the age of the 2800 ± 90 yr. old (Grønlie 1978) cementation of older Holocene fossils in the Båsmoen Mine.

3.9 GPS network

By using differential static GPS (Global Positioning System), it is possible to achieve a relative positioning between two stations, better than a few millimetres over distances of tens to hundreds of kilometres (depending on the type of receiver). We have therefore established a GPS network (Fig. 23) designed to investigate the possible presence of active strain in the Ranafjorden area (Sanderud 1993, Olesen et al. 1993). Three 15-20 km-long profiles are located across outer, central and inner Ranafjorden. The network is expected to give an accuracy of 5-10 mm in the horizontal plane and 15-20 mm in height. Similar networks are already established in Sweden (Talbot & Henkel 1991, Talbot 1992). If there is any active neotectonic deformation in the Ranafjorden area, as indicated by previously published land uplift observations, this should be recorded by GPS in less than a decade.

4 DISCUSSION AND CONCLUSIONS

Based on comparisons between observed seismicity and geodetic levelling, Slunga (1991) claimed that almost all present deformation in the Baltic Shield is aseismic. Most of the movements represent episodic aseismic sliding along crustal faults, and the earthquakes occur when this slip is locked in small segments which then suddenly break. This type of aseismic creep can explain why relatively large-scale deformation in the Rana area may occur without large-magnitude earthquakes. Geodetic and seismological studies in Finland and Sweden have also shown that horizontal movements can be even greater than, or of the same order of magnitude as the vertical block movements (Slunga 1991, Saari 1992)

The nappes consisting mainly of pelitic rocks situated between the tectonic basement windows (Sjona and Høgtuva) to the north and the Bindalen Batholith to the south, are themselves representing a zone of weakness. Contemporary movements along the cleavage of Caledonian phyllites are, for instance, documented by Roberts (1991) along the NW continuation of the postglacial Stuoragurra Fault in the Precambrian of Finnmark.

It is not likely that the observed high annual uplift rates have been constant for several hundreds of thousands of years at the same location. Had this been the case, the result would have been the formation of escarpments, up to a kilometre in height. The most likely situation, on the other hand, is a migration of the active faults and it is also possible that the high uplift rate could be the result of strike-slip faulting.

Another possible indication of neotectonic activity in the Nordland area relates to the discovery of numerous fossils (belemnites) on the shore of Austerdalsvatn in front of the Svartisen glacier in 1960, and described by Grønlie (1973). He suggested that the fossils may have originated from Mesozoic or Tertiary sediments beneath the glacier on the Svartisen plateau. The fossil locality is situated at an altitude of 210 m above sea-level while the Svartisen plateau (ice surface) is situated at an altitude of approximately 1200 m..

The Ranafjorden area is located along the NW continuation of 50 km-wide Precambrian shear zone through central Norrland in Sweden (Henkel & Roslund 1993, Henkel in press). This shear zone may be located below the Caledonian nappes in the Ranafjorden area and therefore constitutes a regional zone of weakness. The NW-SE trending Lofoten lineament (Blystad et al. in press) offshore to the northwest of the Svartisen area may also represent a reactivation of this shear zone.

There are indications of recent faulting in the Ranafjorden area and the adjacent region. It is difficult, however, to find conclusive evidence for both older postglacial and present-day movements along specific faults. We have therefore established a GPS network designed to

investigate the possible presence of active strain in the Ranafjorden area. We will recommend a remeasurement of the net every second year, and also to extend this GPS network into the Svartisen area which is an area of increased earthquake activity. Several hydro-electric power plants are located in this area and the hydro-power company Statkraft have also considered participating in a follow-up project (T. Hoff, pers. comm. 1994).

We would also recommend carrying out more detailed structural mapping along the fault zones, especially the N-S trending normal faults and the eastern and western sections of the Båsmoen Fault which have only been briefly studied in the present work. There is also a need for a mapping of postglacial deformation in the overburden to check if these phenomena are related to the Båsmoen Fault or other faults in the area. Interpretation of aeromagnetic and gravimetric data will provide information on the structural relations at depth between the Precambrian basement and the Caledonian nappes. This information is useful for estimating the depth extent of the Ranafjorden Lineament.

5 ACKNOWLEDGEMENTS

This study has been carried out within NGU's Nordland Programme. Sivert Bakkelid and Per Skjøthaug (the Norwegian Mapping Authority), Hilmar Bungum and Unni Byrkjeland (NORSAR/Univ. of Oslo), and Arne Myrvang and Helge Ruistuen (Norwegian Institute of Technology) have provided information on land uplift data, seismicity and *in situ* stress measurements, respectively, in the Ranafjorden area. Gunnar Grønlie drafted the figures. The Norwegian Petroleum Directorate and the Norwegian Mapping Authority permitted us to use the remeasurement data of the 1894 acorn barnacle and bladder wrack marks. David Roberts has critically read the report and made suggestions towards its improvement. To all these persons and institutions we express our sincere thanks.

6 REFERENCES

- Anundsen, K. 1992: Late Weichselian relative sea levels in southwest Norway: observed strandline tilts and neotectonic activity. *Geol. Fören. Stockh. Förh.* 111, 288-292.
- Atakan, K., Lindholm, C.D. & Havskov, J. 1994: Earthquake swarm in Steigen, northern Norway: an unusual example of intraplate seismicity. *Terra Nova* 6, 180-194.
- Bakkeliid, S. 1989: Innmåling av rur- og tangrandmerker i Finnmark. *Statens kartverk Rapport 4/1989*, 59 pp.
- Bakkeliid, S. 1990: Innmåling av rur- og tangrandmerker i Nordland. *Statens kartverk Rapport 3/1990*, 90 pp.
- Bakkeliid, S. 1991: Innmåling av rur- og tangrandmerker i Troms og Nordland. *Statens kartverk Rapport 2/1991*, 91 pp.
- Bakkeliid, S. 1992: Mapping the rate of crustal uplift in Norway: parameters, methods and results. *Nor. Geol. Tidsskr.* 72, 239-246.
- Blystad, P., Færseth, R.B., Larsen, B.T., Skogseid, J. & Tørudbakken, B. in press.: Structural elements of the Norwegian continental shelf, Part 2. The Norwegian Sea. *Nor. Petr. Dir. Bull.* 6.
- Bungum, H., Alsaker, A., Kvamme, L.B. & Hansen, R.A. 1991: Seismicity and seismotectonics of Norway and nearby continental shelf areas. *Jour. Geophys. Res.* 96, 2249-2265.
- Bungum, H. & Husebye, E.S. 1979: The Meløy, northern Norway, earthquake sequence - a unique intraplate phenomenon. *Nor. Geol. Tidsskr.* 59, 189-193.
- Bungum, H., Hokland, B.K., Husebye, E. & Ringdal, F. 1979: An exceptional intraplate earthquake sequence in Meløy, Northern Norway. *Nature* 280, 32-35.
- Byrkjeland, U. in prep.: *Seismotectonics of the Norwegian Continental Margin 62°-71°N*. Cand. Sci. Thesis, Univ. of Oslo.
- Bäckblom, G. & Stanfors, R. 1989: Interdisciplinary study of post-glacial faulting in the Lansjärv area, northern Sweden, 1986-1988. *Swedish Nuclear Fuel and Waste Management Co. Technical Report 89-31*, 171 pp.
- Bøckman, K.L. 1964: Bergverksdriften i Mo prestegjeld. In Coldevin, A. (ed.), *Mo Prestegjeld etter 1850, Rana bygdebok, Mo Sparebank*, 303-322.
- Foslie, S. 1926: Norske svovelkisforekomster. *Nor. geol. unders.* 127, 122 pp.
- Gabrielsen, R.H. & Ramberg, I.B. 1979a: Fracture patterns in Norway from Landsat imagery: results and potential use. *Proceedings Norwegian Sea Symposium, Tromsø 1979*, Norwegian Petroleum Society, NSS/123, 1-23.
- Gabrielsen, R.H. & Ramberg, I.B. 1979b: Tectonic analysis of the Meløy earthquake area based on Landsat lineament mapping. *Nor. Geol. Tidsskr.* 59, 183-187.
- Gabrielsen, R.H., Ramberg, I.B., Mørk, M.B.E. & Tveiten, B. 1981: Regional geological, tectonic and geophysical features of Nordland, Norway. *Earth evolution sciences* 1, 14-26.

- Grønlie, O.T. 1922: Strandlinjer, moræner og skjælføremster i den sydlige del av Troms fylke. *Nor. geol. unders.* 94, 39 pp.
- Grønlie, O.T. 1923: Har Høgtuva steget i vor tid? *Naturen* 7, 139-141.
- Grønlie, O.T. 1939: Some remarks on the land area in Nordland between the glacier Svartisen, and the frontier. *Nor. Geogr. Tidsskr.* 7, 399-406.
- Grønlie, A. 1973: Fossile blekkspruter funnet ved Svartisen. *Årbok for Rana VI, Rana Museums- og Historielag*, 65-70.
- Grønlie, A. 1978: Fossilfunn i Bossmo Grube. *Årbok for Rana XI, Rana Museums- og Historielag*, 69-78.
- Gustavson, M. & Gjelle, S.T. 1991: Geologisk kart over Norge. Berggrunnskart MO I RANA, M. 1:250 000. *Norges geologiske undersøkelse*.
- Heltzen, I.A. 1834: Ranens Beskrivelse. *Rana Museums- og Historielag, Mo i Rana, 1981*, 290 pp.
- Henkel, H. in press: Shear lenses and steep shear zones in the Baltic Shield. *Tectonophysics*.
- Henkel, H. & Roslund, M. 1993: 1:a ordningens branta skjuvsoner i Sverige. *Swedish Nuclear Fuel and Waste Management Co. Technical Report*
- Hofseth, A. 1939: Foreløpig uttalelse om den geofysiske malmleting ved Bossmo og Malmhaug Gruber - høsten 1939. *NGU Bergarkiv Rapport 1132*, 6 pp.
- Hovland, M. 1985: Carbonate cemented pillars at Nesøya, North Norway: Proposal for an alternative model of formation. *Nor. Geol. Tidsskr.* 65, 221-223.
- Johnsen, E. 1981: Kvartære trekk fra Beiarns geologiske historie. *Årbok for Beiarn, Beiarn historielag. Egil Trohaugs Forlag a.s, Bodø*, 93-106.
- Kujansuu, R. 1964: Nuorista sirroksista Lapissa. Summary: Recent faults in Lapland. *Geologi* 16, 30-36.
- Lagerbäck, R. 1979: Neotectonic structures in northern Sweden. *Geol. Fören. Stockh. Förh.* 100 (1978), 271-278.
- Lagerbäck, R. 1990: Late Quaternary faulting and paleoseismicity in northern Fennoscandia, with particular reference to the Lansjärv area, northern Sweden. *Geol. Fören. Stockh. Förh.* 112, 333-354.
- Lagerbäck, R. 1992: Dating of Late Quaternary faulting in northern Sweden. *Journ. Geol. Soc. London* 149, 285-291.
- Lauritzen, S.E. 1991a: Karst landforms of Norway, 1:500 000, Map sheet 5. *Geological institute, University of Bergen*.
- Lauritzen, S.E. 1991b: Karst landforms of Norway, 1:500 000, Map sheet 6. *Geological institute, University of Bergen*.
- Lundquist, J. & Lagerbäck, R. 1976: The Pärve Fault: A late-glacial fault in the Precambrian of Swedish Lapland. *Geol. Fören. Stockh. Förh.* 98, 45-51.
- Mokhtari, M. 1991: *Geological model for the Lofoten continental margin*. Dr. Scient. Thesis. Univ. of Bergen, Norway, 184 pp.
- Muir Wood, R. 1989: The Scandinavian Earthquakes of 22 December 1759 and 31 August 1819. *Disasters* 12, 223-236.

- Muir Wood, R. 1989: Extraordinary deglaciation reverse faulting in northern Fennoscandia. In S. Gregersen & P.W. Basham (eds.) *Earthquakes at North-Atlantic passive margins: neotectonics and postglacial rebound*. NATO ASI series. Series C, Mathematical and physical sciences, vol. 266. Kluwer Academic Publishers, Dordrecht, The Netherlands, 141-173.
- Muir Wood, R. 1993: A review of the seismotectonics of Sweden. *Swedish Nuclear Fuel and Waste Management Co. Technical Report 93-13*, 225 pp.
- Myrvang, A. 1993: Rock stress and rock stress problems in Norway. In J.A. Hudson (ed.) *Comprehensive rock engineering. Vol. 3, Rock testing and site characterization*. Pergamon Press, 461-471.
- Nagy, J. & Dypvik, H. 1984: Lithified Holocene shallow marine carbonates from Nesøya, North Norway. *Nor. Geol. Tidsskr.* 64, 121-133.
- Nagy, J. & Dypvik, H. 1986: Carbonate cemented pillars on Nesøya: A reply. *Nor. Geol. Tidsskr.* 66, 187-188.
- Nordenskjöld, O. 1895: Om Bossmo grufvors geologi. *Geol. Fören. Stockh. Förh.* 17, 523-542.
- Olesen, O. 1988: The Stuoragurra Fault, evidence of neotectonics in the Precambrian of Finnmark, northern Norway. *Nor. Geol. Tidsskr.* 68, 107-118.
- Olesen, O., Henkel, H., Lile, O.B., Muring, E., & Rønning, J.S. 1992a: Geophysical investigations of the Stuoragurra postglacial fault, Finnmark, northern Norway. *Journ. Applied Geophysics* 29, 95-118.
- Olesen, O., Henkel, H., Lile, O.B., Muring, E., Rønning, J.S. & Torsvik, T.H. 1992b: Neotectonics in the Precambrian of Finnmark, northern Norway. *Nor. Geol. Tidsskr.* 72, 301-306.
- Olesen, O. Henkel, H., Sanderud, Ø. & Skogseth, T. 1993: GPS network to measure active strain along the postglacial Båsmoen Fault in the Ranafjorden area. *Norwegian Geological Society, Tectonic and Structural Geology Studies Group, TSGS-93 meeting 4-5 November 1993, Trondheim, Programme with abstracts*, p 24.
- Olsen, L. 1989: Bæivašgied'di, 2033 III kvartærgeologisk kart. 1:50 000. *Norges geologiske undersøkelse*.
- Roberts, D. 1991: A contemporary small-scale thrust-fault near Lebesbye, Finnmark. *Nor. Geol. Tidsskr.* 71, 117-120.
- Rokoengen, K. & Sættem, J. 1983: Shallow bedrock geology and Quaternary thickness off northern Helgeland, Vestfjorden and Lofoten. *Continental Shelf Institute (IKU) Report P-155/2/83*, 44 pp.
- Saari, J. 1992: A review of the seismotectonics of Finland. *Nuclear Waste Commission of the Finnish Power Companies Report YJT-92-29*, 79 pp.
- Sanderud, Ø. 1993: Analyse av nøyaktighet av GPS til bruk i neotektoniske studier. *Unpubl. thesis. Norwegian Institute of Technology, NTH, Trondheim*, 60 pp.
- Slunga, R. 1991: The Baltic Shield earthquakes. *Tectonophysics* 189, 323-331.

- Sørensen, R., Bakkelid, S. & Torp, B. 1987: Landhevning. 1:5 mill. In: *Nasjonalatlas for Norge. Hovedtema 2: Landformer, berggrunn og løsmasser*. Kartblad 2.3.3. Statens kartverk.
- Søvegjarto, U., Marker, M., Graversen, O. & Gjelle, S. 1988: Berggrunnskart MO I RANA 1927 I - M. 1:50 000. *Norges geologiske undersøkelse*.
- Søvegjarto, U., Marker, M. & Gjelle, S. 1989: Berggrunnskart STORFORSHEI 2027 IV - M. 1:50 000. *Norges geologiske undersøkelse*.
- Søvegjarto, U. 1978: Bossmo grubefelt. Sluttrapport geologi. *Rana Gruber Rapport 78-16*, 29 pp.
- Talbot, C.J. 1992: GPS networks to measure active strains in Sweden. *Geol. Fören. Stockh. Förh.* 114, 378-380.
- Talbot, C.J. & Henkel, H. 1991: Swedish neotectonics by ground positioning satellites: The northern GPS (Lansjärv) profile. Internal University of Uppsala Report, 23 pp.
- Tanner, V. 1930: Studier över kvartärsystemet i Fennoskandias nordliga delar IV. *Bulletin de la Commission Géologique de Finlande* 88, 594 pp.
- Tolgensbakk, J. & Sollid, J.L. 1988: Kåfjord, kvartærgeologi og geomorfologi 1:50 000, 1634 II. *Geografisk institutt, Universitetet i Oslo*.
- Vogt, T. 1923: En postglacial jordskjælvs-forkastning. *Naturen* 7, 65-71.
- Vogt, T. 1939: Rapport over det geologiske arbeide ved Bossmo og Malmhaug malmfelter i Mo i Rana. *NGU Bergarkiv Rapport 1135*, 5 pp.
- Vaage, S. 1980: Seismic evidence of complex tectonics in the Meløy earthquake area. *Nor. Geol. Tidsskr.* 60, 213-217.

List of figures

Fig. 1. Reported Late Quaternary faults in northern Fennoscandia from 1, Grønlie (1922), Vogt (1923); 2, Tanner (1930); 3, Grønlie (1939); 4, Kujansuu (1964); 5, Lundquist & Lagerbäck (1976), Lagerbäck (1979); 6, Rokoengen & Sættem (1983); 7, Olesen (1988); 8, Tolgensbakk & Sollid (1988); 9, Olsen (1989); 10, Mokhtari (1991); 11, Olesen et al. (1992b) and 12, present study. Faults 6,10,11 and 12 are classified as potential Late Quaternary faults since they may also be attributed to other causes (see criteria for classifying postglacial faults in Fennoscandia by Muir Wood (1993)). The present study area is shown by the frame.

Fig. 2. Shaded relief image of the digital topography (100 x 100m grid) from the (A) Helgeland - Salten and the (B) Ranafjorden areas ('illumination' from the east). The location of the Ranafjorden area is shown by the frame in (A).

Fig. 3. Simplified geological map of the Ranafjorden-Svartisen area (Karlsen in prep.)

Fig. 4. Part of the 1:250,000 bedrock geology map Mo i Rana (Gustavson & Gjelle 1991). Potential postglacial faults in the Ranafjorden area and postglacial faults on Kvasshaugen (Grønlie 1939) are added, together with land uplift data (Bakkeliid 1990, 1992). A - Austerdalsvatn, B - Båsmoen, H - Handnesøya, K - Kvasshaugen, L - Litle Alteren, LU - Lurøya, M - Meløy, N - Nesøya, S - Straumbotn, U - Utskarpen.

Fig. 5. Part of the 1:50,000 bedrock geology map Mo i Rana (Søvegjarto et al. 1988). The Båsmoen Fault is added to the map. Same legend as in Fig. 4.

Fig. 6. Late Quaternary faults (Grønlie 1939) and potential Late Quaternary faults (the present study), earthquake epicentres 1987-1993 (Byrkjeland in prep.), focal mechanism solutions (Bungum & Husebye 1979, Vaage 1980, Bungum et al. 1991), in situ stress measurements (Myrvang 1993) and land uplift data (Sørensen et al. 1987, Bakkeliid 1990,1991) in the Helgeland-Svartisen area. A - Austerdalsvatnet, B - Båsmoen, F - Fagervika, H - Hemnesberget, M - Meløy, N - Nesøya, S - Straumbotn, U - Utskarpen. The Late Quaternary fault (Grønlie 1939) south of Beiarn is classified as one of the most reliable claims of neotectonic surface fault rupture in Scandinavia (Muir Wood 1993).

Fig. 7. Effects of the 31 August 1819 earthquake in the epicentral region, around the parishes of Hemnes, Lurøy and Nesna (Muir Wood 1989a).

Fig. 8. Lineament interpretation map of the Straumbotn - Slettefjellet - Alteren area. The Båsmoen Fault (lineament) and an interpretation of profile AB across the fault are also shown.

Fig. 9. (A) Oblique aerial photograph of the Båsmoen Fault crossing the southern part of Straumbotn in the foreground and Slettefjellet in the background; looking east. The uplifted (0.5 m) boathouse was located on the shore of the bay Straumbotn (Fig. 5). The fault is shown by the arrows. (B) Photograph of the Båsmoen Fault scarp on Slettefjellet; looking east. The fault is here split up into two escarpments.

Fig. 10. Detailed structural profile across the Båsmoen Fault on Slettefjellet. The foliation is steeper directly below the escarpment than to the NNW and SSE. This bending of the foliation is interpreted to be associated with an older dip-slip movement. Fractures and small faults with a dip of 40-50° are also observed within the fault zone. The offset of geological boundaries across the Båsmoen Fault is generally small, usually less than 5-10 m. The southern block is interpreted to be uplifted during the Late Quaternary.

Fig. 11. Observed mesoscopic structures in the Straumbotn - Båsmoen area. (A) Pie-sliced rose diagram showing the trends of faults, $n = 37$. (B) Pie-sliced rose diagram showing the trends of joints, $n = 81$. (C) Stereoplot (lower hemisphere) of poles to joints ($n = 81$, contoured with an isoline interval of 1.23 %) and faults (stars) in bedrock and normal faults (triangles) in postglacial overburden.

Fig. 12. Observed mesoscopic structures in the bay Utskarpen, (A) Pie-sliced rose diagram showing the trends of faults, $n = 9$. (B) Pie-sliced rose diagram showing the trends of joints, $n = 16$. (C) Stereoplot (lower hemisphere) of poles to faults (stars, $n = 9$) and joints (squares, $n = 16$).

Fig. 13. Aerial photograph of the Båsmoen Fault on Båsmofjellet. The fault, shown by the arrows, is trending ENE-WSW and cuts the strike of the bedding (c. NE-SW) at an angle of approximately 20° . The southern block seems to be uplifted. The Båsmoen Mine is located along the continuation of the fault immediately to the east of the picture. A number of small lineaments parallel to the Båsmoen Fault trend can also be seen on the photograph.

Fig. 14. Oblique aerial photograph of the Båsmoen Fault on Båsmofjellet, looking east, approximately 4 km to the west of the centre of Mo i Rana in the background of the picture. The fault is shown by the arrows. The continuation of the BF across Loftfjellet to the east of Båsmoen can be seen in the background.

Fig. 15. Photograph of the same escarpment as shown in Figs. 13 and 14; looking WSW. The height of the escarpment on Båsmofjellet varies between 1 and 30 m. Some of this escarpment uplift, however, formed before the deglaciation, since ice striae are locally observed where the escarpment is at its highest.

Fig. 16. Photographs from the escarpment of the Båsmoen Fault on Båsmofjellet. (A) Disc-shaped lenses of schist can locally be observed in the escarpment and are thought to have been formed during postglacial faulting. (B) A rock-slide occurred in the escarpment during the summer of 1993.

Fig. 17. Oblique aerial photograph of the Båsmoen-Yttern area, looking WNW. Ranafjorden can be seen to the bottom left. A farmhouse on Enge (E) located within the Båsmoen Fault was uplifted approximately 1 m in the 1870's relative to the mountains Høgtuva (H) and Snøfjellet (S). B - Båsmoen Mine (open pit).

Fig. 18. Storstrand farm in the bay Utskarpen, looking east. The depression located between the shore and the forest to the right was caused by the landslide triggered by the magnitude 5.8-6.2 earthquake in 1819 (Heltzen 1834, Muir Wood 1989). The scarps of the landslide are shown by the arrows. The bay to the left in the photograph was filled up with sediments so that boats could not come to the shore. An uplift of this shallow sea floor above sea-level occurred during an aftershock in 1819. Muir Wood (1989) ascribed this phenomenon to piling up of material behind a rotational slump in the marine clay. This is difficult to conceive, however, since the landslide terminated against the bedrock escarpment (to the right in the picture). Utskarpen is situated within the Båsmoen Fault and fault scarps are situated 200 m to the south (right) and 300 m to the north (left) of the landslide. The uplift of the sea floor in 1819 could therefore have been caused by movements along these faults.

Fig. 19. Several vertical normal faults cutting the glacial morphology on Handnesøya looking northwards from the quay at Nesna. These faults are interpreted as possible Riedel shears to the Båsmoen Fault. The western blocks are down-faulted.

Fig. 20. Aerial photograph of NNE-SSW trending normal faults to the south of Austerdalsvatn (Fig. 4) cutting the glacial morphology. Minor NNW-SSE trending normal faults can also be seen. The faults are shown by the arrows.

Fig. 21. Corrugations in fine-grained sand from Fagervika, 20 km to the northeast of Sandnessjøen. The sand was deposited after the deglaciation. Similar structures occur close to the Lansjärv postglacial fault in northern Sweden (Lagerbäck 1990).

Fig. 22. (A) Faulted sediments of interpreted postglacial age in the Litle Alteren area 400 m to the north of the Båsmoen Fault. The synthetic faults are listric and the antithetic faults make up horsts and grabens in the hanging-wall blocks. The large fault to the right of the centre of the picture is also listric and soles out in the marine clay below the silt and sand. (B) Close-up photograph of the framed area in the picture above. Convolutions in sandy and silty layers.

Fig. 23. Layout of the GPS network in the Ranafjorden area.

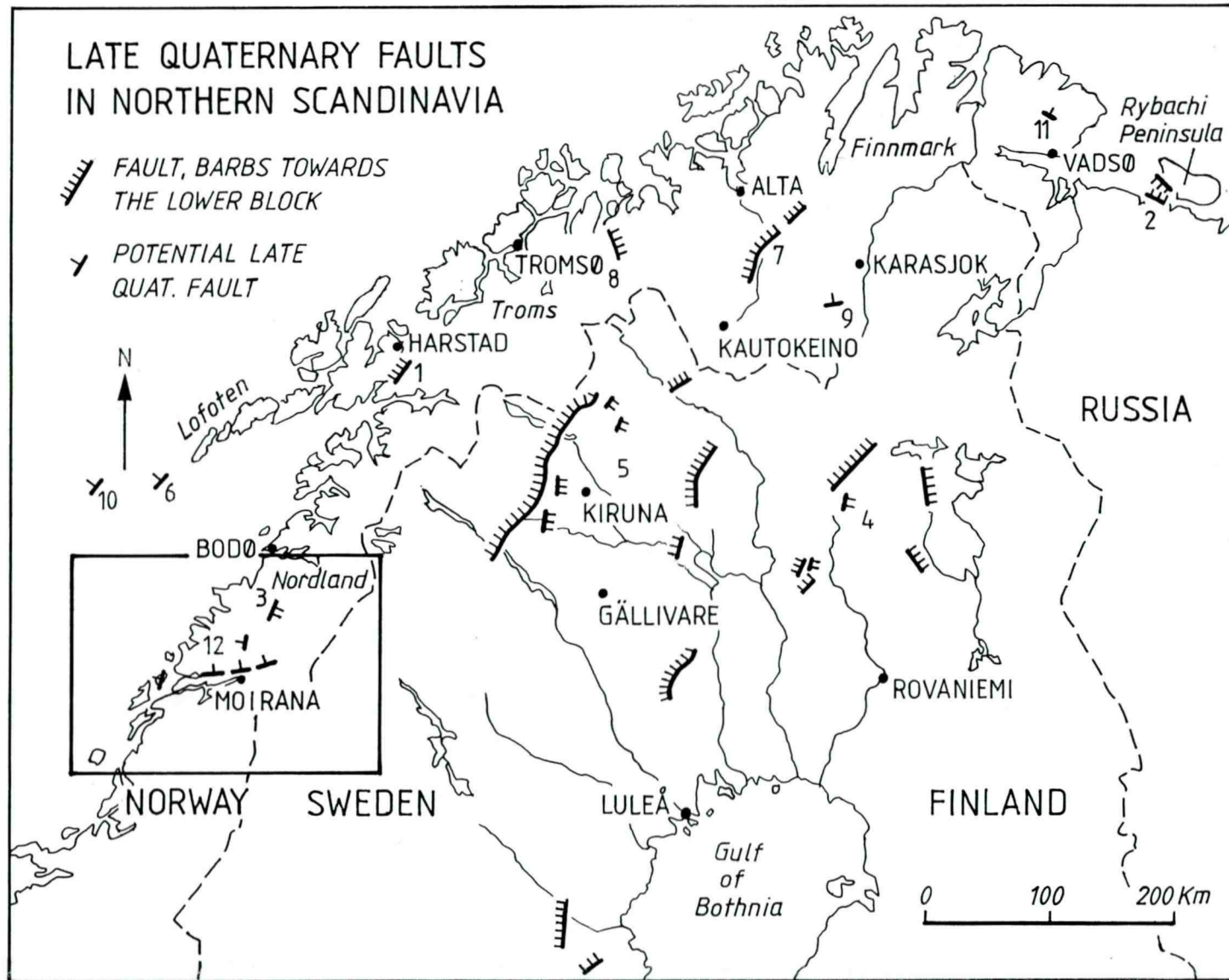


Fig. 1. Reported Late Quaternary faults in northern Fennoscandia from 1, Grønlie (1922), Vogt (1923); 2, Tanner (1930); 3, Grønlie (1939); 4, Kujansuu (1964); 5, Lundquist & Lagerbäck (1976), Lagerbäck (1979); 6, Rokoengen & Sættem (1983); 7, Olesen (1988); 8, Tolgensbakk & Sollid (1988); 9, Olsen (1989); 10, Mokhtari (1991); 11, Olesen et al. (1992b) and 12, present study. Faults 6, 10, 11 and 12 are classified as potential Late Quaternary faults since they may also be attributed to other causes (see criteria for classifying postglacial faults in Fennoscandia by Muir Wood (1993)). The present study area is shown by the frame.

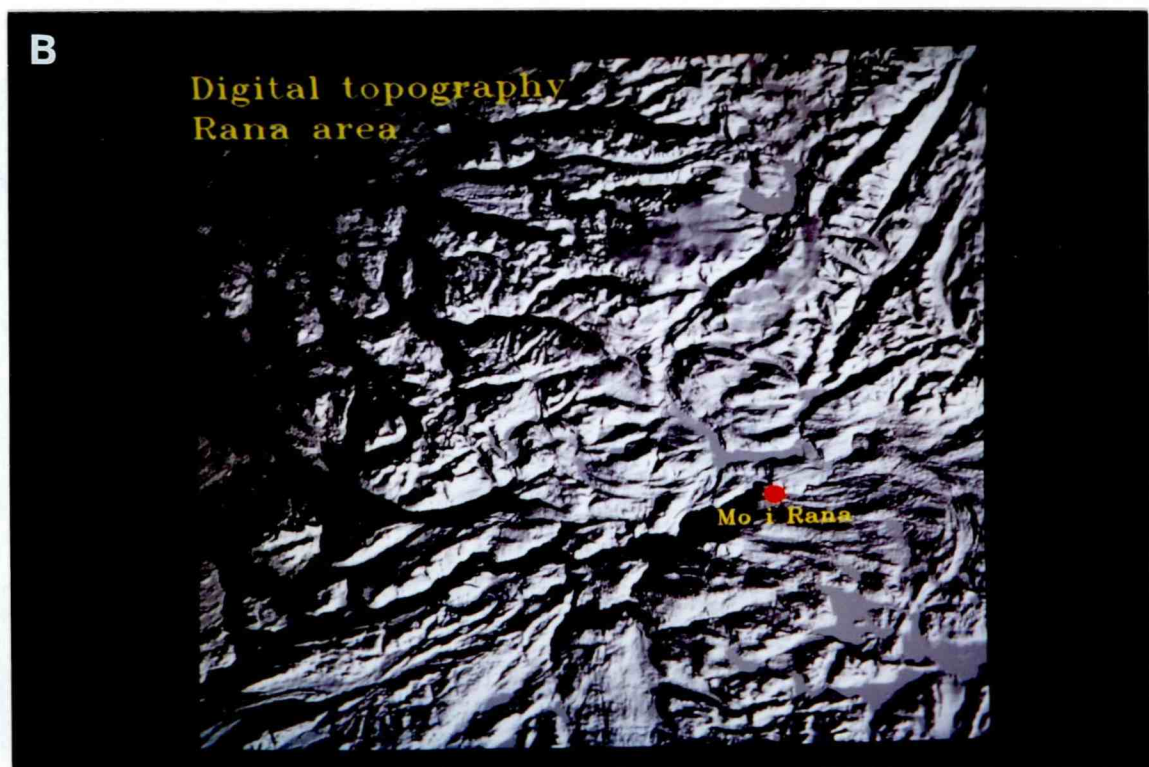
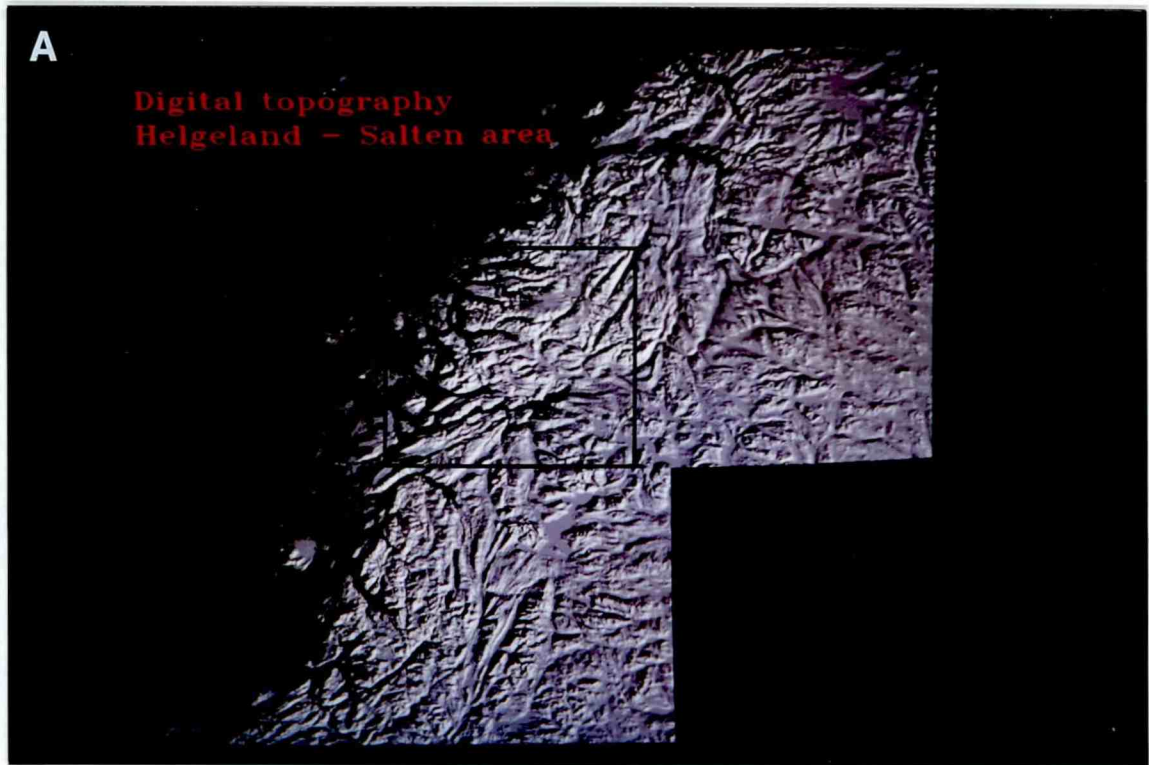


Fig. 2. Shaded relief image of the digital topography (100 x 100m grid) from the (A) Helgeland - Salten and the (B) Ranafjorden areas ('illumination' from the east). The location of the Ranafjorden area is shown by the frame in (A).

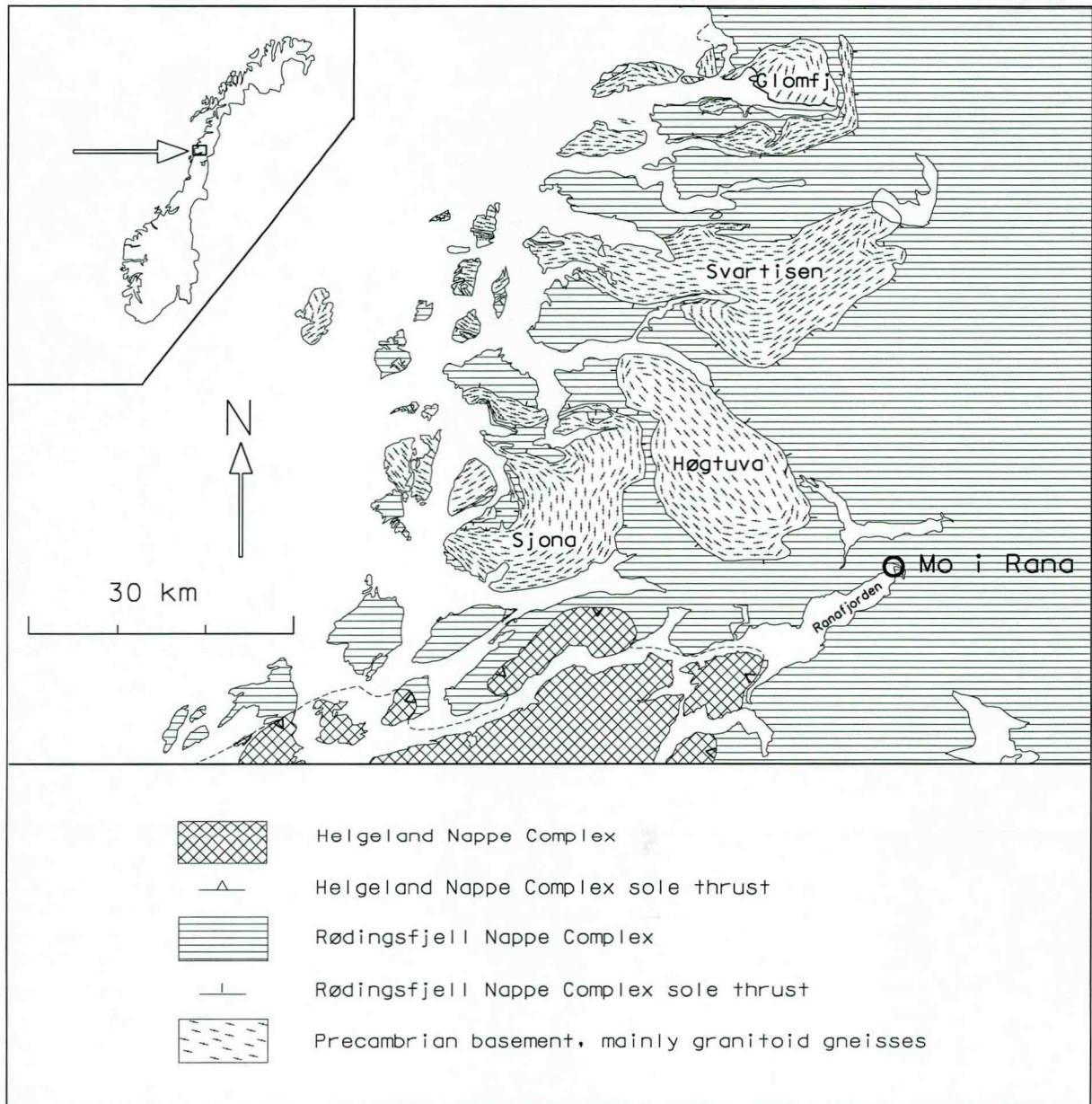


Fig. 3. Simplified geological map of the Ranafjorden-Svartisen area (Karlsen in prep.)

LATE QUATERNARY FAULTS RANAFJORD AREA

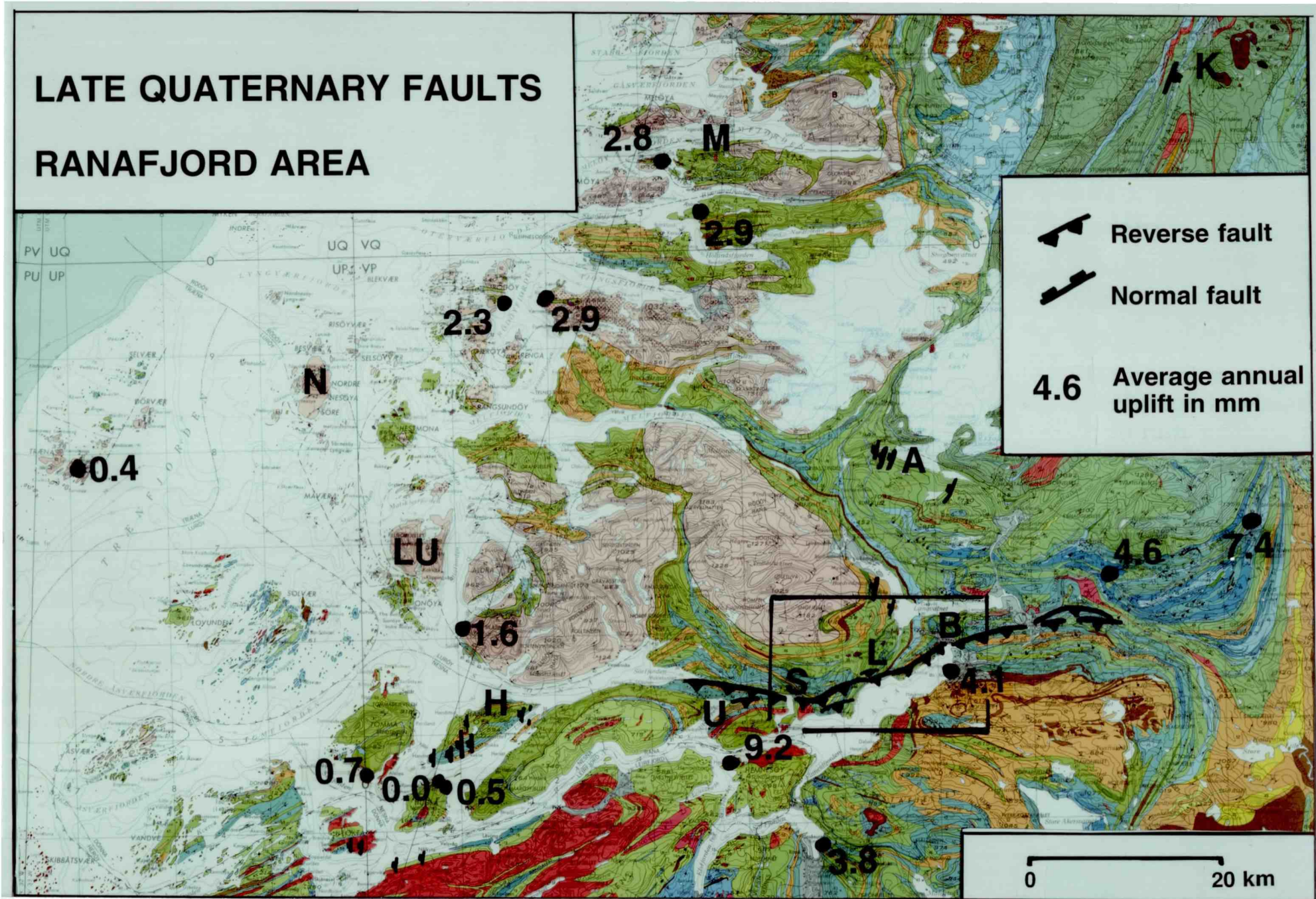


Fig. 4. Part of the 1:250,000 bedrock geology map Mo i Rana (Gustavson & Gjelle 1991). Potential postglacial faults in the Ranafjorden area and postglacial faults on Kvasshaugen (Grønlie 1939) are added, together with land uplift data (Bakkeliid 1990, 1992). A - Austerdalsvatn, B - Båsmoen, H - Handnesøya, K - Kvasshaugen, L - Litle Alteren, LU - Lurøya, M - Meløy, N - Nesøya, S - Straumbotn, U - Utskarpen.

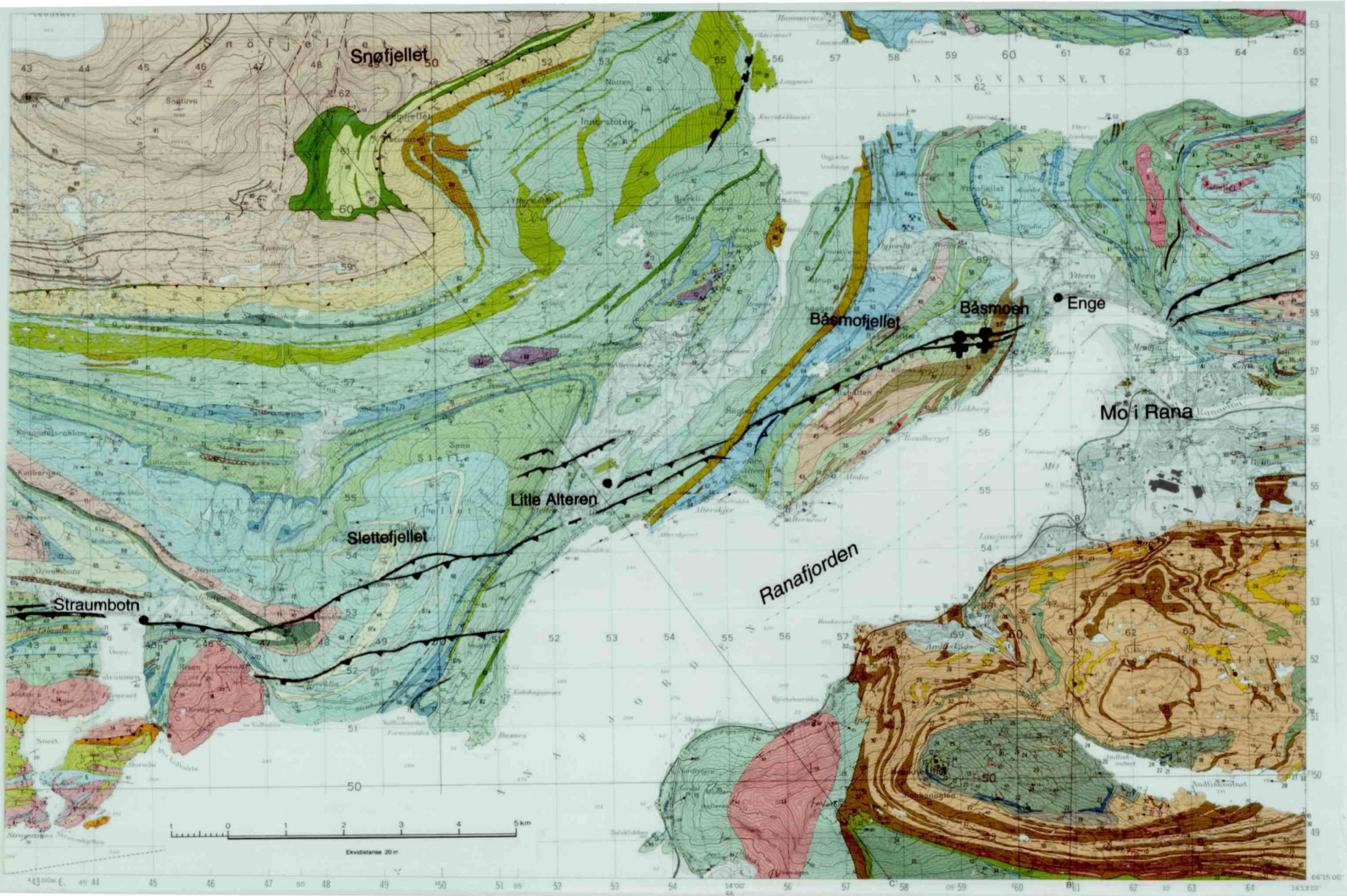


Fig. 5. Part of the 1:50,000 bedrock geology map Mo i Rana (Søvegjarto et al. 1988). The Båsmoen Fault is added to the map. Same legend as in Fig. 4.

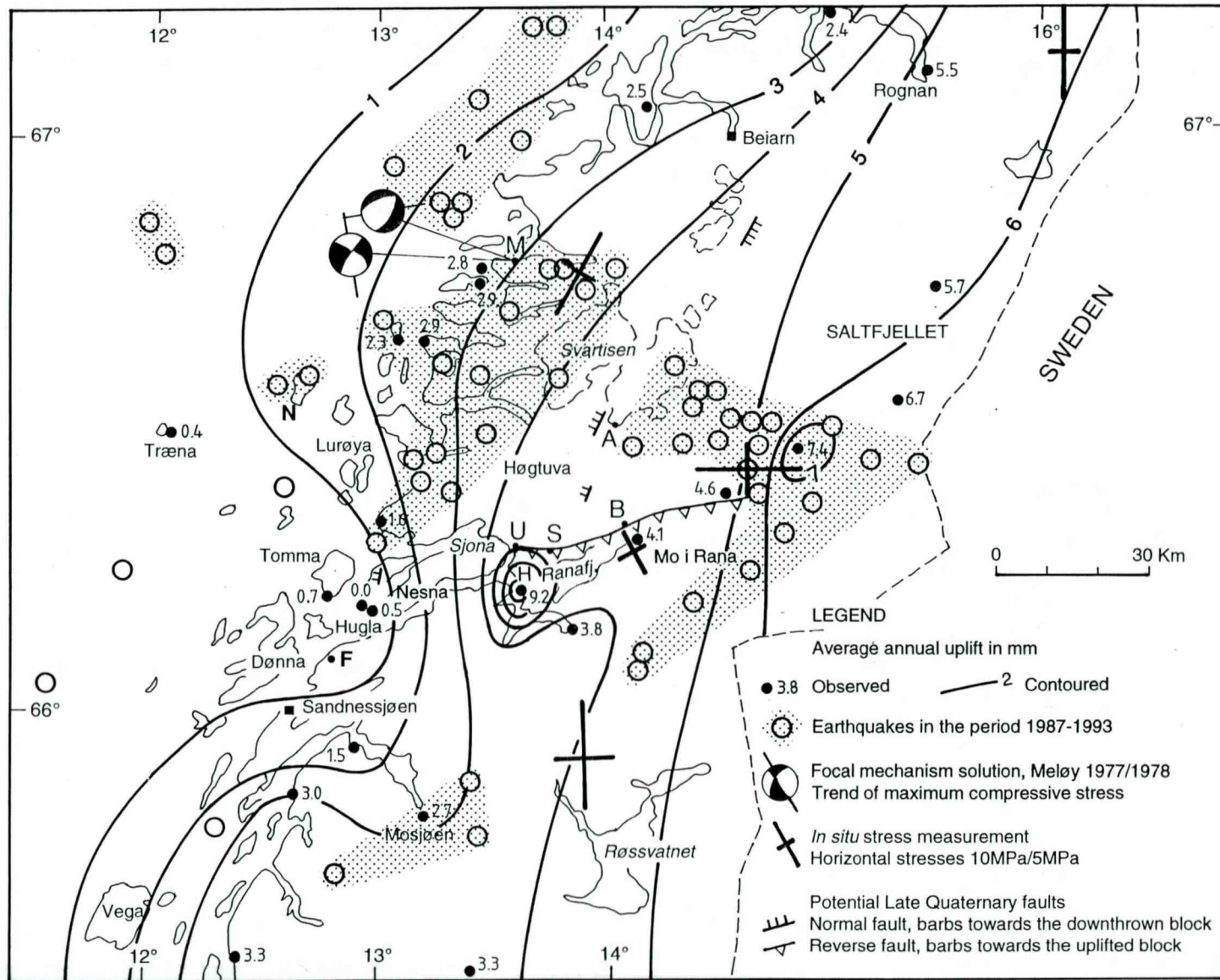


Fig. 6. Late Quaternary faults (Grønlie 1939) and potential Late Quaternary faults (the present study), earthquake epicentres 1987-1993 (Byrkjeland in prep.), focal mechanism solutions (Bungum & Husebye 1979, Vaage 1980, Bungum et al. 1991), in situ stress measurements (Myrvang 1993) and land uplift data (Sørensen et al. 1987, Bakkelid 1990, 1991) in the Helgeland-Svartisen area. A - Austerdalsvatnet, B - Båsmoen, F - Fagervika, H - Hemnesberget, M - Meløy, N - Nesøya, S - Straumbotn, U - Utskarpen. The Late Quaternary fault (Grønlie 1939) south of Beiarn is classified as one of the most reliable claims of neotectonic surface fault rupture in Scandinavia (Muir Wood 1993).

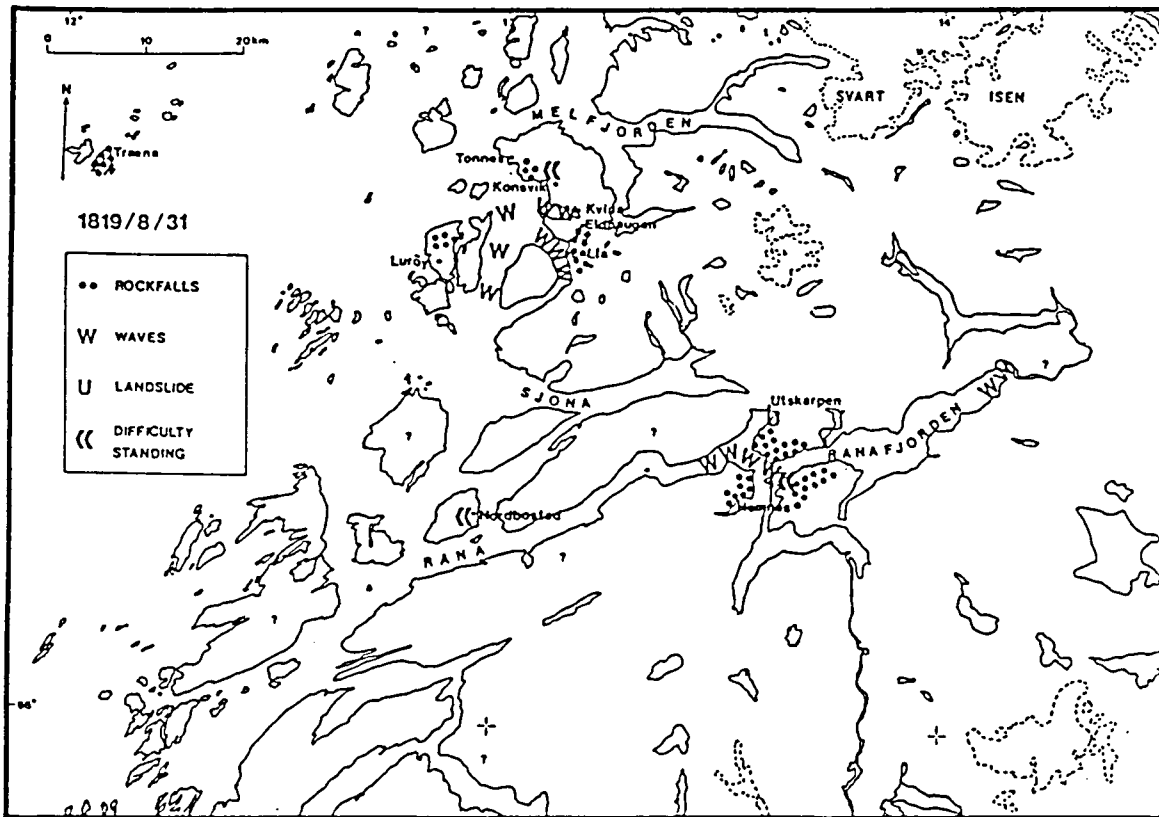


Fig. 7. Effects of the 31 August 1819 earthquake in the epicentral region, around the parishes of Hennes, Lurøy and Nesna (Muir Wood 1989a).

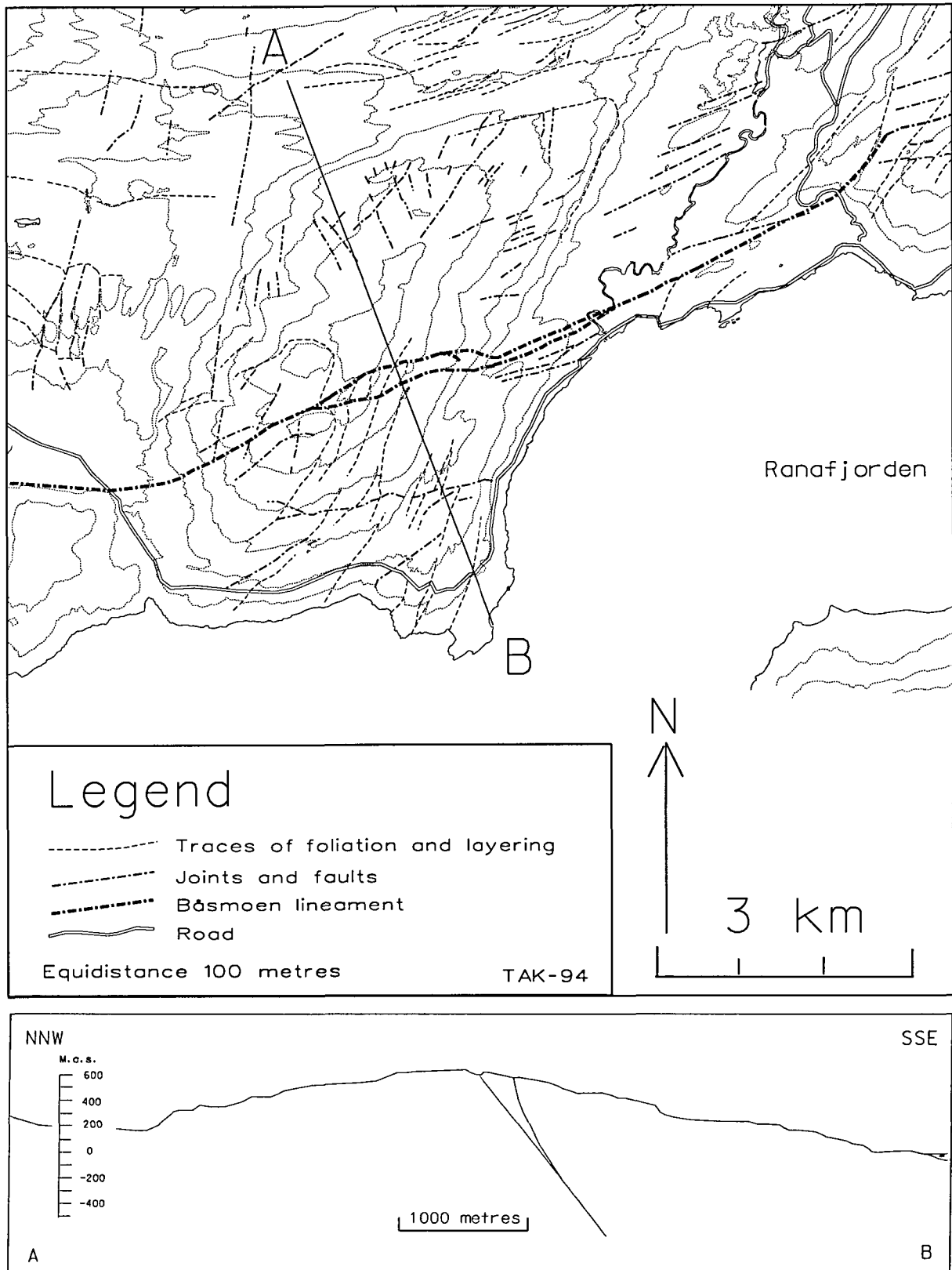


Fig. 8. Lineament interpretation map of the Straumbotn - Slettefjellet - Alteren area. The Båsmoen Fault (lineament) and an interpretation of profile AB across the fault are also shown.



Fig. 9. (A) Oblique aerial photograph of the Båsmoen Fault crossing the southern part of Straumbotn in the foreground and Slettefjellet in the background; looking east. The uplifted (0.5 m) boathouse was located on the shore of the bay Straumbotn (Fig. 5). The fault is shown by the arrows. (B) Photograph of the Båsmoen Fault scarp on Slettefjellet; looking east. The fault is here split up into two escarpments.

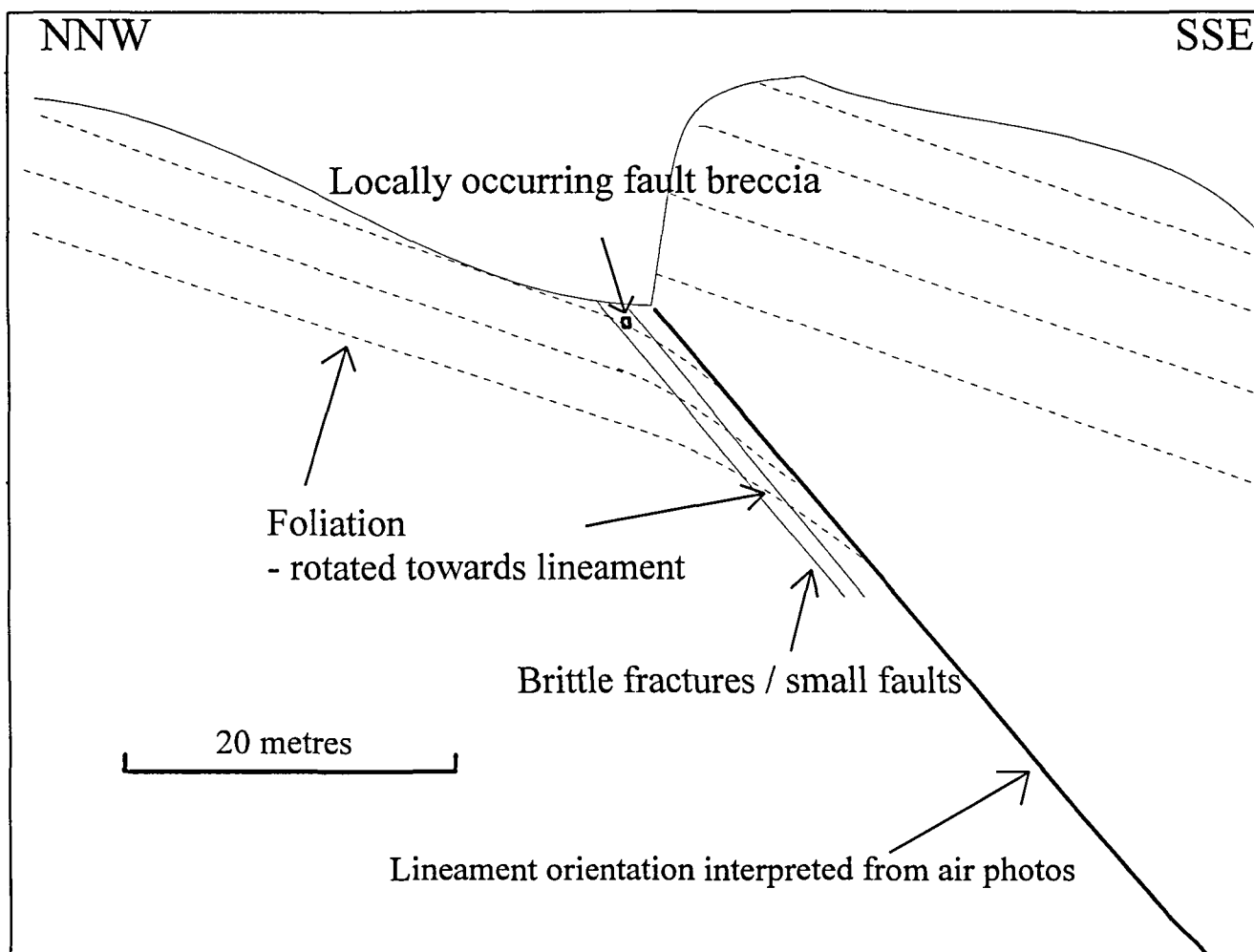


Fig. 10. Detailed structural profile across the Båsmoen Fault on Slettefjellet. The foliation is steeper directly below the escarpment than to the NNW and SSE. This bending of the foliation is interpreted to be associated with an older dip-slip movement. Fractures and small faults with a dip of 40-50° are also observed within the fault zone. The offset of geological boundaries across the Båsmoen Fault is generally small, usually less than 5-10 m. The southern block is interpreted to be uplifted during the Late Quaternary.

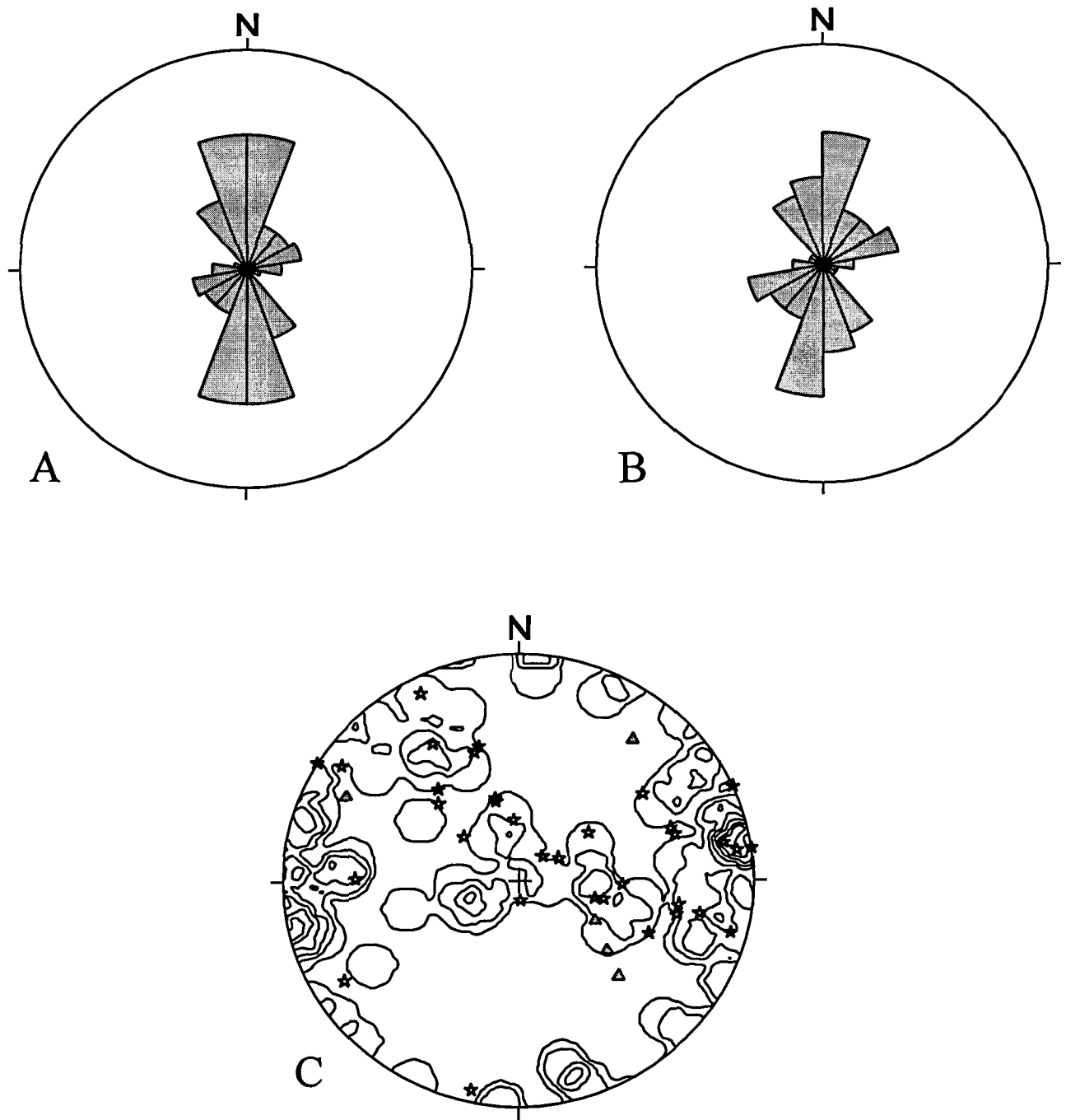


Fig. 11. Observed mesoscopic structures in the Straumbotn - Båsmoen area. (A) Pie-sliced rose diagram showing the trends of faults, $n = 37$. (B) Pie-sliced rose diagram showing the trends of joints, $n = 81$. (C) Stereoplot (lower hemisphere) of poles to joints ($n = 81$, contoured with an isoline interval of 1.23 %) and faults (stars) in bedrock and normal faults (triangles) in postglacial overburden.

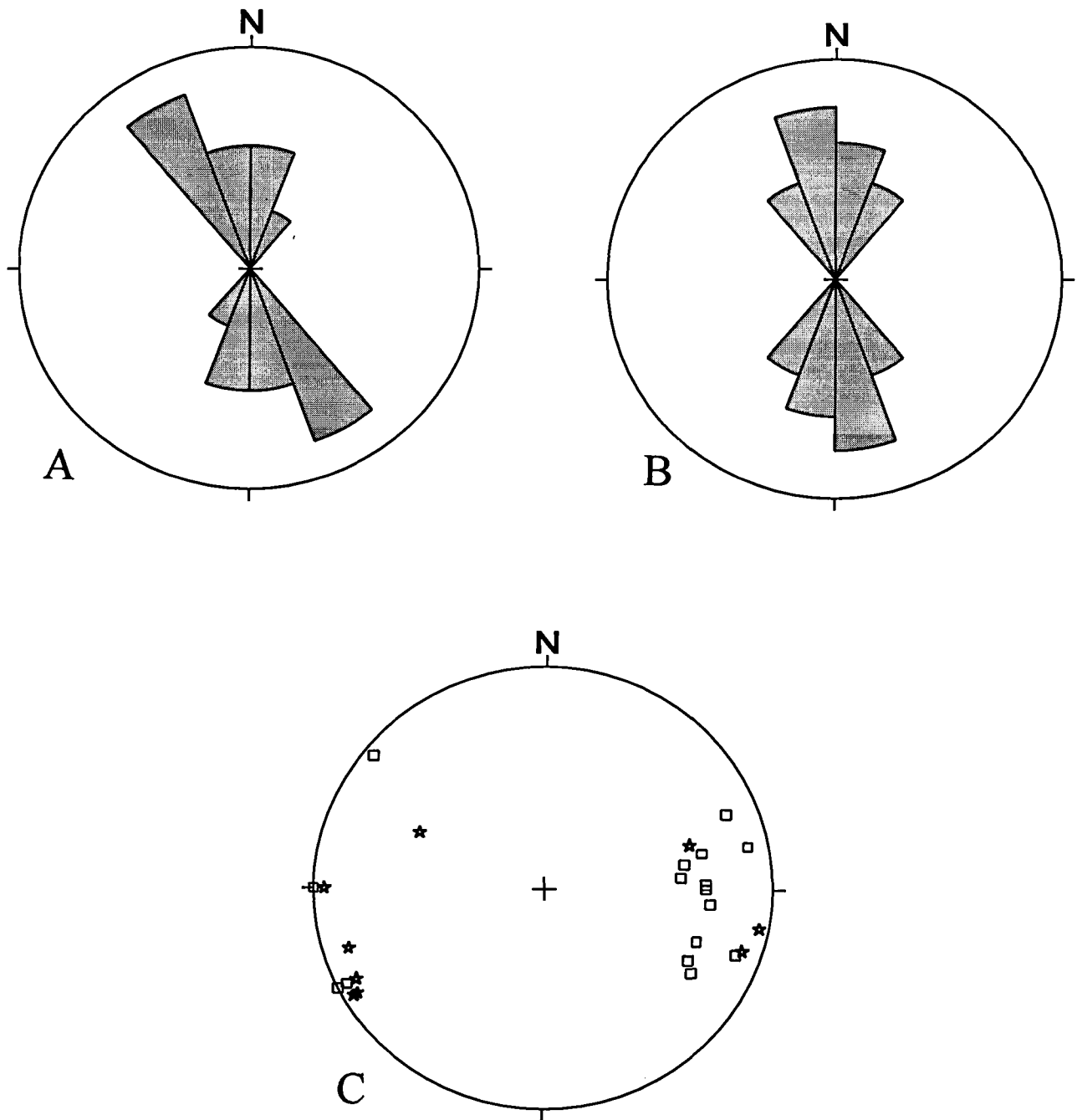


Fig. 12. Observed mesoscopic structures in the bay Utskarpen, (A) Pie-sliced rose diagram showing the trends of faults, $n = 9$. (B) Pie-sliced rose diagram showing the trends of joints, $n = 16$. (C) Stereoplot (lower hemisphere) of poles to faults (stars, $n = 9$) and joints (squares, $n = 16$).



Fig. 13. Aerial photograph of the Båsmoen Fault on Båsmofjellet. The fault, shown by the arrows, is trending ENE-WSW and cuts the strike of the bedding (c. NE-SW) at an angle of approximately 20° . The southern block seems to be uplifted. The Båsmoen Mine is located along the continuation of the fault immediately to the east of the picture. A number of small lineaments parallel to the Båsmoen Fault trend can also be seen on the photograph.



Fig. 14. Oblique aerial photograph of the Båsmoen Fault (BF) on Båsmofjellet, looking east, approximately 4 km to the west of the centre of Mo i Rana in the background of the picture. The fault is shown by the arrows. The continuation of the BF across Loftfjellet to the east of Båsmoen can be seen in the background.



Fig. 15. Photograph of the same escarpment as shown in Figs. 13 and 14; looking WSW. The height of the escarpment on Båsmofjellet varies between 1 and 30 m. Some of this escarpment uplift, however, formed before the deglaciation, since ice striae are locally observed where the escarpment is at its highest.



Fig. 16. Photographs from the escarpment of the Båsmoen Fault on Båsmoffjellet. (A) Disc-shaped lenses of schist can locally be observed in the escarpment and are thought to have been formed during postglacial faulting. (B) A rock-slide occurred in the escarpment during the summer of 1993.



Fig. 17. Oblique aerial photograph of the Båsmoen-Yttern area, looking WNW. Ranaffjorden can be seen to the bottom left. A farmhouse on Enge (E) located within the Båsmoen Fault was uplifted approximately 1 m in the 1870's relative to the mountains Høgtuva (H) and Snøfjellet (S). B - Båsmoen Mine (open pit).



Fig. 18. Storstrand farm in the bay Utskarpen, looking east. The depression located between the shore and the forest to the right was caused by the landslide triggered by the magnitude 5.8-6.2 earthquake in 1819 (Heltzen 1834, Muir Wood 1989). The scarps of the landslide are shown by the arrows. The bay to the left in the photograph was filled up with sediments so that boats could not come to the shore. An uplift of this shallow sea floor above sea-level occurred during an aftershock in 1819. Muir Wood (1989) ascribed this phenomenon to piling up of material behind a rotational slump in the marine clay. This is difficult to conceive, however, since the landslide terminated against the bedrock escarpment (to the right in the picture). Utskarpen is situated within the Båsmoen Fault and fault scarps are situated 200 m to the south (right) and 300 m to the north (left) of the landslide. The uplift of the sea floor in 1819 could therefore have been caused by movements along these faults.



Fig. 19. Several vertical normal faults cutting the glacial morphology on Handnesøya looking northwards from the quay at Nesna. These faults are interpreted as possible Riedel shears to the Båsmoen Fault. The western blocks are down-faulted.

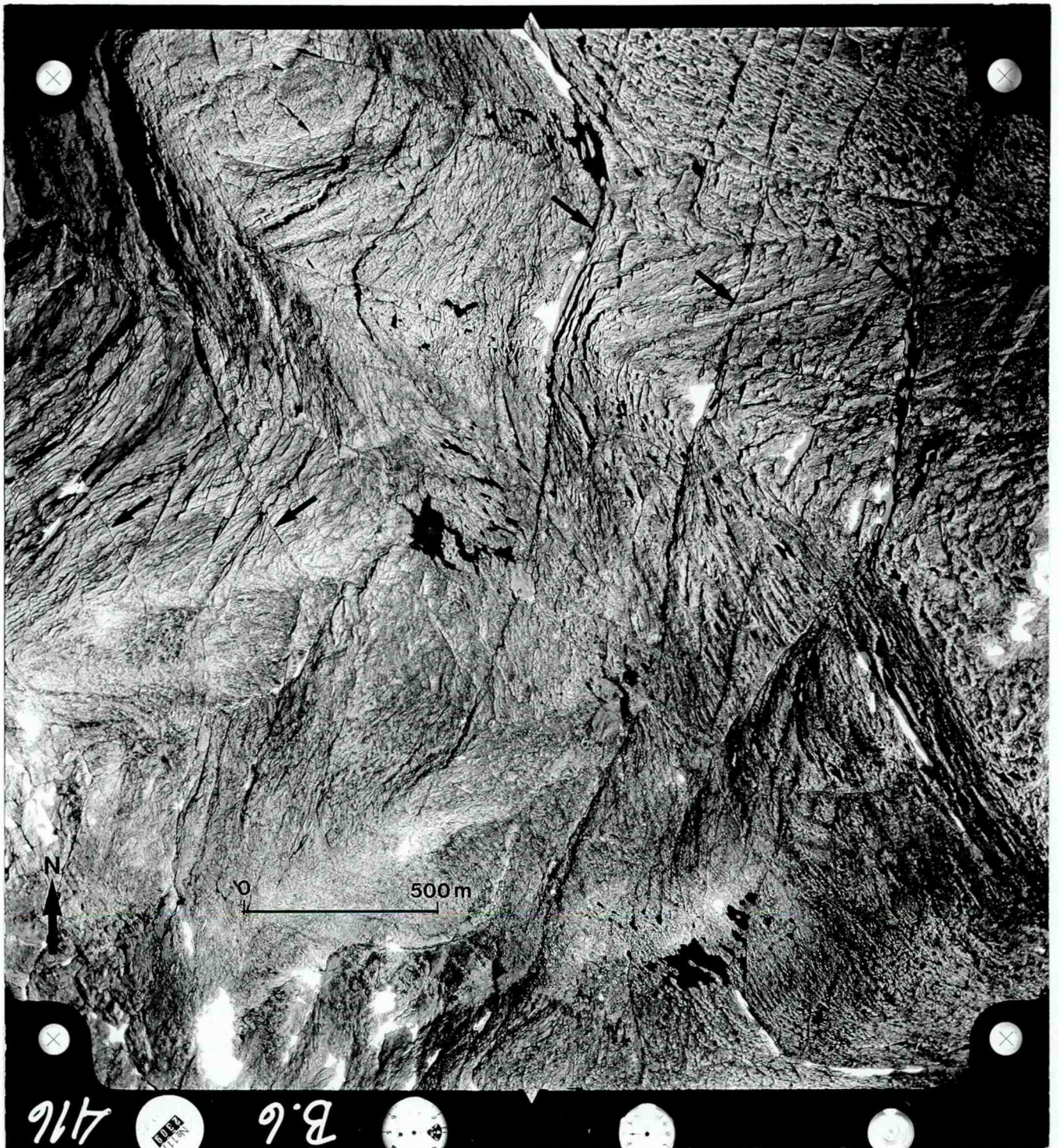


Fig. 20. Aerial photograph of NNE-SSW trending normal faults to the south of Austerdalsvatn (Fig. 4) cutting the glacial morphology. Minor NNW-SSE trending normal faults can also be seen. The faults are shown by the arrows.



Fig. 21. Corrugations in fine-grained sand from Fagervika, 20 km to the northeast of Sandnessjøen. The sand was deposited after the deglaciation. Similar structures occur close to the Lansjärv postglacial fault in northern Sweden (Lagerbäck 1990).

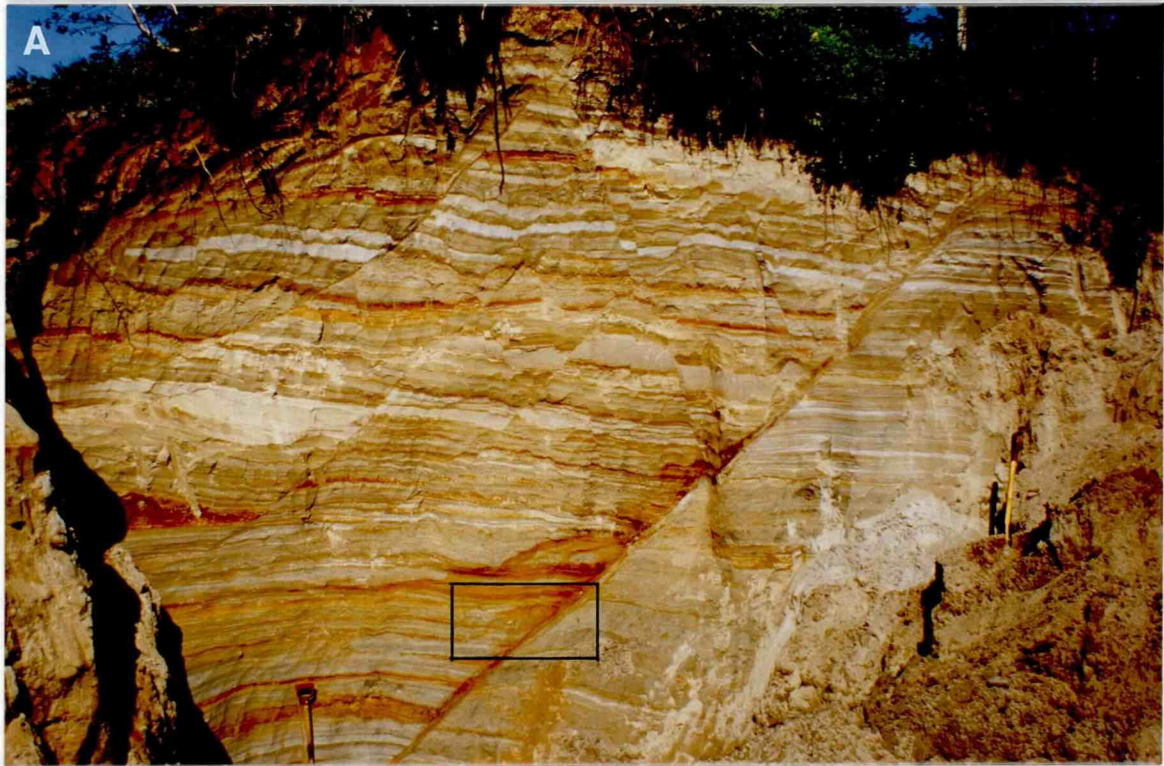


Fig. 22. (A) *Faulted sediments of interpreted postglacial age in the Litle Alteren area 400 m to the north of the Båsmoen Fault. The synthetic faults are listric and the antithetic faults make up horsts and grabens in the hanging-wall blocks. The large fault to the right of the centre of the picture is also listric and soles out in the marine clay below the silt and sand.* (B) *Close-up photograph of the framed area in the picture above. Convolutions in sandy and silty layers.*

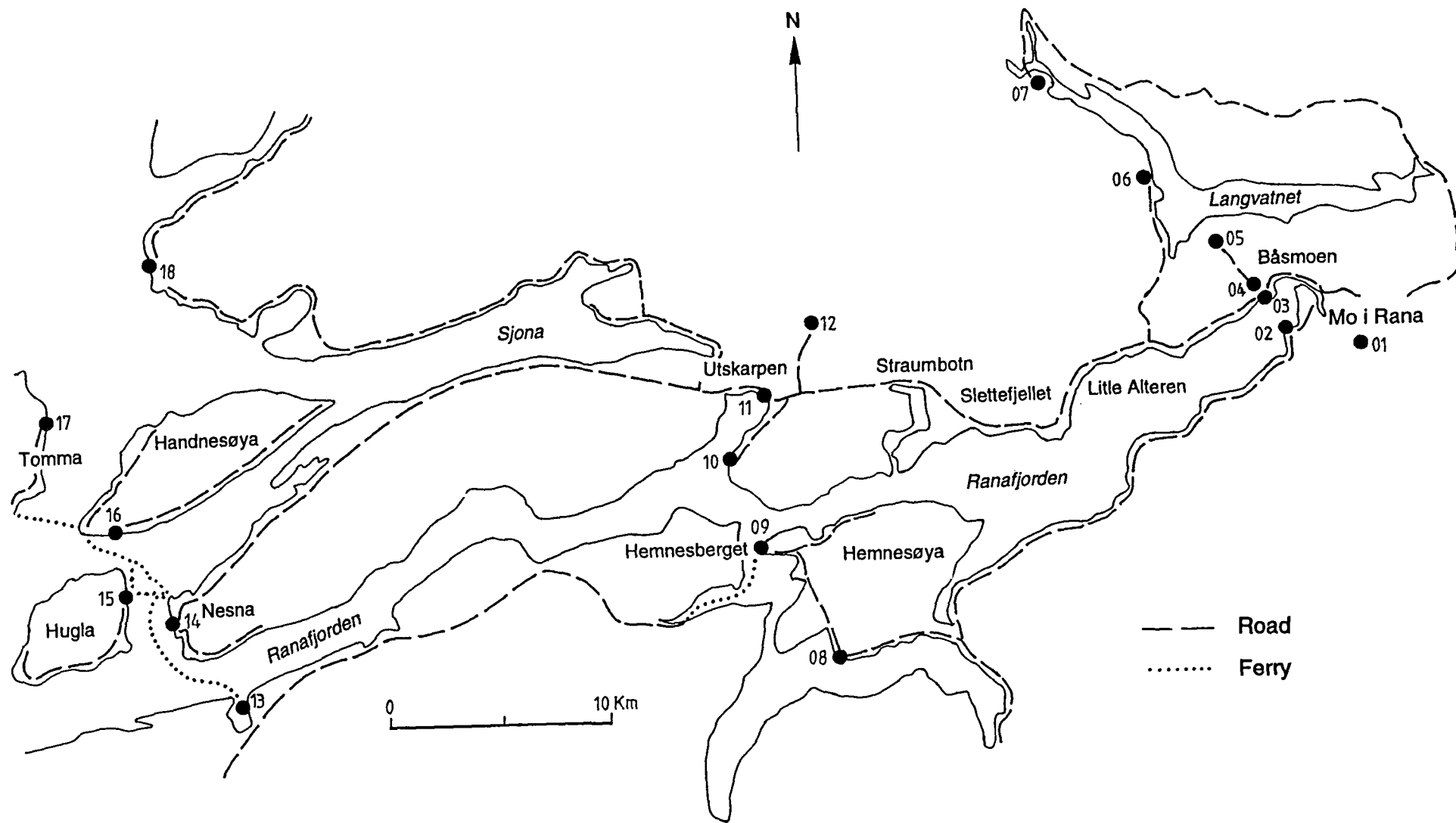


Fig. 23. Layout of the GPS network in the Ranafjorden area.